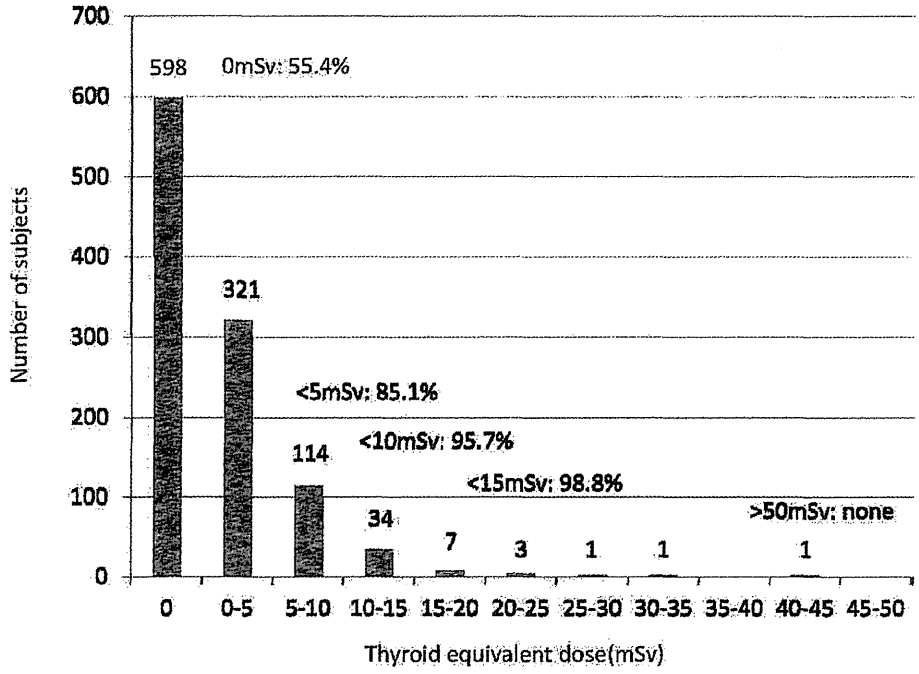

FIG. 5. Distribution of thyroid equivalent doses estimated by the results of the screening survey and the intake scenario from March 12, 2011 to the day before measurements.

on the neck of examinees. They found detectable ^{131}I activity in 39 of the 45 people evacuated from coastal areas, and in 7 of the 17 residents in Tsushima District (Namie Town). Thyroid equivalent doses by inhalation ranged from none detected to 33 mSv (*19*). The median thyroid equivalent doses for children and adults were 4.2 and 3.5 mSv, respectively.

Internal Doses Evaluated by WBC

Internal contamination with radionuclides in the whole body was also a concern for residents in Fukushima Prefecture; therefore, the Fukushima prefectural government monitored internal radionuclide contamination in residents. A preliminary study of 174 residents was

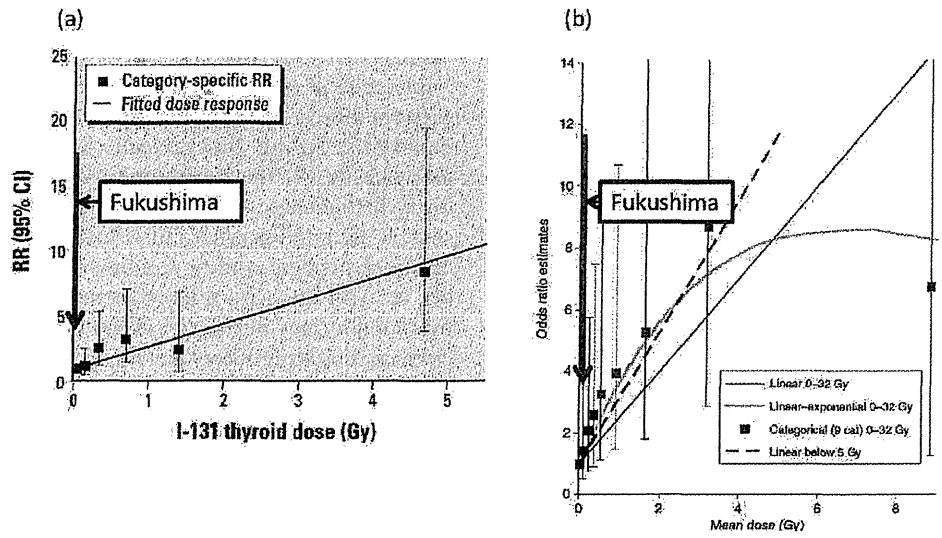

FIG. 6. Panel a: Thyroid radiation doses in Fukushima, Ukraine and Belarus in dose-response relationship between thyroid cancer and ^{131}I. Panel b: Dose-response relationship for the incidence of thyroid cancers. Both figures were modified from two articles (republished with permission, Brenner AV, et al. *Environ Health Perspect* 2011;119:933–9 and Zablotska LB, et al. *Br J Cancer* 2011;104:181–7).

TABLE 3
Whole-Body Dose of Residents in Fukushima Prefecture

Dose	Number of residents
<1 mSv	118,904
1 mSv	14
2 mSv	10
3 mSv	2
Total	118,930

Notes. Whole-body doses were calculated based on the assumption that ^{134}Cs and ^{137}Cs were inhaled on March 12, 2011, for residents measured at the end of January 2012, or ingested continuously from March 12, 2011, for those measured afterward. This assumption was made so as not to underestimate the doses of residents. The results contain no serial measurement in the same person. The results are as of February 2013 and are available on the Fukushima Prefecture website (*19*).

performed at the NIRS in Chiba. The internal doses calculated were <1 mSv in all residents.

Fukushima Prefecture subsequently announced the results of internal radiation doses measured from June 2011 to February 2013. The total number of subjects, consisting of Fukushima Prefecture residents and evacuees in Niigata Prefecture was 118,930. Of these, 118,904 (99.9%) showed values of a committed effective dose (a measure of health effects on an individual due to an intake of radioactive material into their body) that was <1 mSv and the maximum was 3 mSv in two people (*20*) (Table 3).

The Minamisoma City office also monitored the internal doses of students at 579 primary/junior high schools, 4,745 high schools and in adults by whole-body counter (WBC) at the Minamisoma City General Hospital from September 26 to December 27, 2011 (*21*). The office reported the results on their website. This study was performed independently of other organizations, and one adult had 1.1 mSv as a committed effective dose, while the doses of the students and other adults were <1 mSv.

Tsubokura *et al.* evaluated the ^{137}Cs body burdens of 1,432 children and 8,066 adults by WBC in Minamisoma City, 23 km from the Fukushima Daiichi Nuclear Power Plant, and reported low-exposure levels in most adults and children tested (*22*). Values were much lower than those reported in studies years after the Chernobyl accident (49 Bq/kg after 7–10 years). Hayaho *et al.* also carried out a WBC survey in 32,811 people between October 2011 and November 2012, and showed that the ^{137}Cs body burdens of all children ($n = 1,383$) were below the detection limit of 300 Bq/body in the fall of 2012 (*23*).

At Nagasaki University, Nagasaki Prefecture, Matsuda *et al.* measured internal radioactivity by WBC in evacuees and short-term visitors to Fukushima within one month after the accident, and reported that ^{131}I, ^{134}Cs and ^{137}Cs were detected in more than 30% of examined individuals, at maximum committed doses and thyroid equivalent doses of 1 and 20 mSv, respectively (*24*).

DISCUSSION

The World Health Organization (WHO) recently assessed public health risks due to the Fukushima Daiichi Nuclear Power Plant accident and reported that the two most affected locations of Fukushima Prefecture showed preliminary estimated radiation effective doses for the first year ranging from 12–25 mSv (*25*). The WHO also estimated that the lifetime risks are predicted to increase to around 7% for leukemia in males exposed as infants; for thyroid cancer, the estimated lifetime risk increases to around 70% in females exposed as infants. However, these estimates are based on the assumption that people in the most affected areas outside the 20-km radius continued to live there for four months after the accident (*26*).

Countermeasures at the outset of the accident were carried out according to the radiation dose calculated from the readings at the monitoring posts. These countermeasures considered several assumptions from the point of view of protection and safety. Evacuation was planned to avoid an external exposure of >20 mSv/year and food was strictly controlled to limit internal exposure. In this article, we reviewed the screening results of thyroid equivalent doses in the initial phase of the accident in Iitate Village, Kawamata Town and Iwaki City, and showed that 95.7% of the children received <10 mSv, with a maximum of 35 mSv, which is lower than the intervention level (50 mSv) (*15, 16*). Thyroid equivalent doses around Chernobyl have been extensively estimated. Zablotska *et al.* estimated individual thyroid doses in Belarus based on individual thyroid activity measurements and dosimetric data from questionnaires (*18*). They estimated that thyroid doses ranged from nearly 0–32.8 Gy, with an arithmetic mean of 0.56 Gy, which were much higher than those in Fukushima. This suggests that compared to Chernobyl, the countermeasures at the outset of the accident in Fukushima effectively minimized the internal radiation exposure to the thyroid gland.

Information about individual radiation doses is now accumulating, and the exploratory committee of the Fukushima Health Management Survey has indicated on its web site (*9*) that radiation from the accident will not likely be the cause of health effects in the future. Based on several assumptions, the individual radiation doses experienced by residents during the first 4 months of the accident are very different from those estimated by the readings of the monitoring posts. A clear difference between the ambient dose equivalent and the individual dose rate has been reported by Yoshida *et al.* (*27*).

In any event, sincere scientific efforts must be continued to obtain individual radiation doses that are as accurate as possible. However, the protocol for determining the health effects of radiation has to be reevaluated to observe the health effects due to individual radiation doses (e.g., external doses <5 mSv/first 4 months, internal doses <1 mSv/year and thyroid doses <35 mSv). Dose-responsiveness is crucial and collecting sufficient data to confirm the

presence or absence of radiation health effects should be the aim of the survey.

In particular, the schedule of decontamination should be reconsidered. The current decontamination map is based on the results of airborne monitoring, and the radiation dose is calculated from the readings at the monitoring posts taken during the initial period of the accident. The decontamination protocol should be reconsidered to account for the individual doses of people who desire to live in those areas.

All stakeholders must consider the relationship between the estimated health effects and the consequences of countermeasures such as evacuation, resettlement, food control, decontamination and health examinations. The goal of countermeasures is to minimize the suffering of exposed residents and to promote recovery from the overall damage of the nuclear accident, the earthquake, and the tsunami.

ACKNOWLEDGMENTS

The authors would like to thank Dr. Nobuhiko Horioka of the Cabinet Office, Nuclear Emergency Response Headquarters, Support Team for Residents Affected by Nuclear Incidents, Health Management Section, for his valuable assistance in collecting reports from the websites of various municipal governments in Fukushima Prefecture and for coordinating the analysis of the reports.

Received: March 2, 2013; accepted: July 26, 2013; published online: October 18, 2013

REFERENCES

1. Editorial. Critical mass. Nature 2011; 480:291.
2. Investigation Committee on the Accident at the Fukushima Nuclear Power Stations of Tokyo Electric Power Company. http://www.cas.go.jp/jp/seisaku/icanps/eng/
3. The National Diet of Japan Fukushima Nuclear Accident Independent Investigation Commission. http://warp.da.ndl.go.jp/info:ndljp/pid/3856371/naiic.go.jp/en/report/
4. The Independent Investigation Commission on the Fukushima Nuclear Accident. http://rebuildjpn.org/en/fukushima/
5. Report of Japanese Government to the IAEA Ministerial Conference on Nuclear Safety - The accident at TEPCO's Fukushima Nuclear Power Stations. http://www.kantei.go.jp/foreign/kan/topics/201106/iaea_houkokusho_e.html
6. Yasumura S, Hosoya M, Yamashita S, Kamiya K, Abe M, Akashi M, Kodama K, Ozasa K. Fukushima Health Management Survey Group. Study protocol for the Fukushima Health Management Survey. J Epidemiol 2012; 22:375–83.
7. Agenda of the fifth reviewing board meeting of Fukushima Prefectural Health Survey (in Japanese). http://www.pref.fukushima.jp/imu/kenkoukanri/240125shiryou.pdf
8. The second report on the overview of Fukushima Prefectural Health Survey (in Japanese). http://www.pref.fukushima.jp/imu/kenkoukanri/240220gaiyo.pdf
9. The tenth report on the overview of Fukushima Prefectural Health Survey (in Japanese). http://www.pref.fukushima.jp/imu/kenkoukanri/250213siryou1.pdf
10. Report on the measurement of individual doses in Date City (in Japanese). http://www.city.date.fukushima.jp/kouhou/pdf-rinzi/rinzi45.pdf
11. Results of citizens' radiation doses in Nihonmatsu City (in Japanese). http://www.city.nihonmatsu.lg.jp/uploaded/attachment/10014.pdf
12. Monitoring results of radioactivity and radiation doses in Tamura City (in Japanese). http://www.city.tamura.lg.jp/uploaded/attachment/2118.pdf
13. The first report on the measurement of individual accumulated doses in Koriyama City (in Japanese). http://www.city.koriyama.fukushima.jp/upload/1/3421_sekisansenryou1.pdf
14. Agenda of the sixth reviewing board meeting of Fukushima Prefectural Health Survey (in Japanese). http://www.pref.fukushima.jp/imu/kenkoukanri/240426shiryou.pdf
15. Kim E, Kurihara O, Suzuki T, Matsumoto M, Fukutsu K, Yamada Y, et al. Screening survey on thyroid exposure for children after the Fukushima Daiichi nuclear power plant station accident. In: Kurihara O, Akahane K, Fukuda S, Miyahara N, Yonai S, editors. Proceedings of the 1st NIRS symposium on reconstruction of early internal dose in the TEPCO Fukushima Daiichi nuclear power station accident; 2012; Jul 10–11; Chiba, Japan: National Institute of Radiological Sciences; 2012.
16. Evaluation on the results of thyroid dose screening in Fukushima Prefecture (in Japanese). http://www.nsr.go.jp/archive/nsc/ad/pdf/hyouka.pdf
17. Brenner AV, Tronko MD, Hatch M, Bogdanova TI, Oliynik VA, Lubin JH, et al. I-131 dose response for incident thyroid cancers in Ukraine related to the Chornobyl accident. Environ Health Perspect 2011;119:933–9.
18. Zablotska LB, Ron E, Rozhko AV, Hatch M, Polyanskaya ON, Brenner AV, et al. Thyroid cancer risk in Belarus among children and adolescents exposed to radioiodine after the Chornobyl accident. Br J Cancer 2011; 104:181–7.
19. Tokonami S, Hosoda M, Akiba S, Sorimachi A, Kashiwakura I, Balanov M. Thyroid doses for evacuees from the Fukushima Nuclear accident. Sci Rep 2012; 2:1–4.
20. Operational situation of examination of internal radiation doses by whole body counter in Fukushima Prefecture (in Japanese). http://wwwcms.pref.fukushima.jp/pcp_portal/PortalServlet?CONTENTS_ID=26211&DISPLAY_ID=DIRECT&NEXT_DISPLAY_ID=U000004.
21. Evaluation of internal radiation doses by whole body counter in Minami-Soma City, Fukushima Prefecture (in Japanese). http://www.city.minamisoma.lg.jp/index.cfm/10,2023,61,html
22. Tsubokura M, Gilmour S, Takahashi K, Oikawa T, Kanazawa Y. Internal radiation exposure after the Fukushima nuclear power plant disaster. JAMA 2012; 308:669–70.
23. Hayano RS, Tsubokura M, Miyazaki M, Satou H, Sato K, Masaki S, Sakuma Y. Internal radiocesium contamination of adults and children in Fukushima 7 to 20 months after the Fukushima NPP accident as measured by extensive whole-body-counter surveys. Proc Jpn Acad Ser B Phys Biol Sci 2013; 89:157–63.
24. Matsuda N, Kumagai A, Ohtsuru A, Morita N, Miura M, Yoshida M, et al. Assessment of internal radiation doses in Fukushima by a whole body counter within one month after the nuclear power plant accident. Rad Res 2013;179:663–8.
25. World Health Organization. Health risk assessment from the nuclear accident after the 2011 Great East Japan earthquake and tsunami, based on a preliminary dose estimation. Geneva: World Health Organization; 2013. pp. 1–172.
26. World Health Organization. Preliminary dose estimation from the nuclear accident after the 2011 Great East Japan Earthquake and Tsunami. Geneva: World Health Organization; 2012. pp. 1–120.
27. Yoshida K, Hashiguchi K, Taira Y, Matsuda N, Yamashita S, Takamura N. Importance of personal dose equivalent evaluation in Fukushima in overcoming social panic. Radiat Prot Dosimetry 2012; 151:144–6.

6930–6941 Nucleic Acids Research, 2013, Vol. 41, No. 14 Published online 30 May 2013
doi:10.1093/nar/gkt467

A novel interplay between the Fanconi anemia core complex and ATR-ATRIP kinase during DNA cross-link repair

Junya Tomida[1], Akiko Itaya[1,2], Tomoko Shigechi[1,3], Junya Unno[1], Emi Uchida[1], Masae Ikura[4], Yuji Masuda[5], Shun Matsuda[6], Jun Adachi[7], Masahiko Kobayashi[8], Amom Ruhikanta Meetei[9], Yoshihiko Maehara[3], Ken-ichi Yamamoto[8], Kenji Kamiya[10], Akira Matsuura[11], Tomonari Matsuda[6], Tsuyoshi Ikura[4], Masamichi Ishiai[1] and Minoru Takata[1,*]

[1]Department of Late Effects Studies, Laboratory of DNA Damage Signaling, Kyoto University, Kyoto 606-8501, Japan, [2]Japan Society for the Promotion of Science (JSPS), Tokyo 102-0083, Japan, [3]Department of Surgery and Science, Graduate School of Medical Sciences, Kyushu University, Fukuoka, 812-8582, Japan, [4]Department of Mutagenesis, Laboratory of Chromatin Dynamics, Radiation Biology Center, Kyoto University, Kyoto 606-8501, Japan, [5]Department of Genome Dynamics, Research Institute of Environmental Medicine, Nagoya University, Nagoya 464-8601, Japan, [6]Research Center for Environmental Quality Management, Kyoto University, Otsu, Shiga 520-0811, Japan, [7]Laboratory of Proteome Research, Proteome Research Center, National Institute of Biomedical Innovation, Ibaraki, Osaka 567-0085, Japan, [8]Department of Molecular Pathology, Cancer Research Institute, Kanazawa University, Kanazawa, Ishikawa 920-0934, Japan, [9]Division of Experimental Hematology and Cancer Biology, Cincinnati Children's Research Foundation and University of Cincinnati College of Medicine, Cincinnati, OH 45229, USA, [10]Department of Experimental Oncology, Research Institute for Radiation Biology and Medicine, Hiroshima University, Hiroshima 734-8553, Japan and [11]Department of Nanobiology, Graduate School of Advanced Integration Science, Chiba University, Chiba 263-8522, Japan

Received April 1, 2013; Revised May 3, 2013; Accepted May 7, 2013

ABSTRACT

When DNA replication is stalled at sites of DNA damage, a cascade of responses is activated in the cell to halt cell cycle progression and promote DNA repair. A pathway initiated by the kinase Ataxia teleangiectasia and Rad3 related (ATR) and its partner ATR interacting protein (ATRIP) plays an important role in this response. The Fanconi anemia (FA) pathway is also activated following genomic stress, and defects in this pathway cause a cancer-prone hematologic disorder in humans. Little is known about how these two pathways are coordinated. We report here that following cellular exposure to DNA cross-linking damage, the FA core complex enhances binding and localization of ATRIP within damaged chromatin. In cells lacking the core complex, ATR-mediated phosphorylation of two functional response targets, ATRIP and FANCI, is defective. We also provide evidence that the canonical ATR activation pathway involving RAD17 and TOPBP1 is largely dispensable for the FA pathway activation. Indeed DT40 mutant cells lacking both RAD17 and FANCD2 were synergistically more sensitive to cisplatin compared with either single mutant. Collectively, these data reveal new aspects of the interplay between regulation of ATR-ATRIP kinase and activation of the FA pathway.

INTRODUCTION

Fanconi anemia (FA) is a hereditary disorder characterized by cancer susceptibility and hypersensitivity to inducers of DNA interstrand cross-links (ICLs) (1,2). FA is caused by mutations in a genetically and biochemically complex set of proteins, including an FA core E3 ligase complex containing eight FA gene products (i.e. FANCA, B, C, E, F, G, L, M) and other associated proteins (i.e. FAAP100, FAAP24, FAAP20) (1,2). The FANCM–FAAP24 subcomplex is thought to load the

*To whom correspondence should be addressed. Tel: +81 75 763 7563; Fax: +81 75 753 7564; Email: mtakata@house.rbc.kyoto-u.ac.jp
Present address:
Junya Tomida, Department of Molecular Carcinogenesis, The University of Texas MD Anderson Cancer Center, Smithville, TX 78957, USA.

rest of the core complex onto damaged chromatin (3,4). The core complex mediates monoubiquitination of the ID complex composed with FANCD2 and FANCI proteins. The monoubiquitinated ID complex in turn recruits the DNA repair nuclease FAN1 (2,5–7), and might function as histone chaperone during ICL repair (8). In addition, it has been suggested that the core complex might have other functions (9). Specific mutations of some additional FA genes (*FANCD1/BRCA2*, *FANCJ/BRIP1*, *FANCN/PALB2*, *FANCO/RAD51C*) are found in familial breast cancer (2,10–12), but these genes and a novel FA gene *FANCP/SLX4* (13,14) do not affect the core signaling pathway, resulting in monoubiquitination of the ID complex. Slx4 is shown to be recruited by monoubiquitinated FANCD2 (15) and contributes to ICL repair mainly through regulation of XPF-ERCC1 nuclease (16).

A critical DNA damage response pathway is mediated by the checkpoint kinase ATR and its protein partner ATRIP. One connection between the FA pathway and ATRIP has been uncovered previously: the checkpoint kinase ATR-ATRIP controls multiple phosphorylation events on FANCI, which trigger FA pathway activation (17–20). ATR kinase activation proceeds in two largely independent steps (21–23): first, a stalled DNA replication fork generates a stretch of single-stranded DNA (ssDNA) covered by Replication protein A (RPA) complex, which in turn recruits ATRIP-ATR into distinct focal areas within cell nuclei. Interaction of RPA-bound ATRIP-ATR with the TOPBP1 protein leads to execution of the S-phase checkpoints. The latter step also involves the specialized RAD9-RAD1-HUS1 (9-1-1) checkpoint clamp and the RAD17-RFC clamp loader (21–23), but the molecular details of these processes are unclear.

We wished to clarify how ATR signaling and the FA pathway are coordinated. We examined the ATR signaling events in FA cell lines, and found that the FA core complex does not simply lie downstream of ATR, but functions in ATR kinase activation after replication stress by enhancing chromatin binding of ATRIP. Unexpectedly, we also found that the canonical ATR activation pathway involving RAD17 and TOPBP1 is largely dispensable for activation of the FA pathway. Taken together, our current data provide novel insights regarding the interplay between ATR-ATRIP kinase and activation of the FA pathway.

MATERIALS AND METHODS

Cell culture, gene targeting and transfection in DT40 cells

Wild-type (WT) and various mutant chicken DT40 cells were cultured in RPMI-1640 medium supplemented with 10% fetal calf serum (FCS), 1% chicken serum, 2 mM L-glutamine, 50 μM 2-mercaptoethanol and penicillin/streptomycin in a 5% CO_2 incubator at 39.5°C. Generation of *rad17*, *atm*, *fancd2*, *fancc*, *fancl*, *fancl* complemented with Green fluorescence protein (GFP)-chFANCL cell lines has been described previously (24–28). *FANCM*-deficient DT40 cells (29), *FANCM* D203A 'knock-in' cells (30), *uspl* (31) and *ube2t* knockout (32) cell lines were kindly provided by Dr K.J. Patel (Cambridge University).

Full-length chicken ATRIP cDNA was amplified by reverse transcriptase polymerase chain reaction (PCR) from DT40 RNA and cloned into pDONR vector (Invitrogen). After sequencing, the gateway system (Invitrogen) was used to transfer the cDNAs to the GFP expression vector (20). Targeting vectors were constructed by subcloning PCR-amplified genomic fragments on both sides of the resistance gene cassettes. All transfections in DT40 were done as described (17).

FANCI K525R 'knock-in' was achieved in a heterozygous *FANCI* knockout clone (17), and the resistance gene cassette flanked by the flippase recognition target (FRT) sites introduced into intron was removed by flippase (FLP) recombinase-mediated excision (Flp expression plasmid was provided by Dr Kyoji Horie, Osaka University). Briefly, cells were transiently transfected with a plasmid encoding FLP recombinase and IRES-puro, and excised cells were isolated by puromycin selection for 2 days followed by limiting dilution. While *fanci*-K525R cells could not monoubiquitinate FANCI, they showed a partial defect in FANCD2 monoubiquitination on DNA damage by mitomycin C (MMC), and displayed only mild sensitivity to cisplatin compared with *fanci* null cells. Conditional *FANCD2* knockout cells were made by knock-in targeting of two FRT sites in *FANCD2* heterozygous knockout clone. The FRT sites flanked a genomic segment that included the exon containing the monoubiquitination site. The resistance gene cassettes were removed by expression of Cre recombinase using plasmid-based transfection. In this conditional cell line, *FANCD2* gene could be inactivated by FLP-mediated excision. *RAD17* gene was targeted in the conditional *FANCD2* knockout cells using RAD17 targeting vector previously described (25).

Human cell cultures and transfections

Human ATRIP-GFP or FANCL-Flag expression vector was constructed by cloning PCR product from HeLa cell cDNA into appropriate expression vectors. GFP-human FAAP100 was similarly made by PCR from a plasmid (a kind gift from Dr Weidong Wang).

Human HeLa S3 cells were maintained in Dulbecco's modified Eagle's medium (DMEM) supplemented with 10% FCS and penicillin/streptomycin in a 5% CO_2 incubator at 37°C, and were introduced with retroviral bicistronic expression vector encoding FLAG-HA-tagged human ATRIP (FLAG-HA-ATRIP) and IRES-CD25 as described (33). The retrovirus was packaged using 293P cells, which were maintained in DMEM supplemented with 10% newborn calf serum and penicillin/streptomycin. The transduced cells were selected on the basis of CD25 expression using Dynabeads (33).

GM6914 (FA-A) with or without complementation with FANCA (a gift from Dr Takayuki Yamashita, Gunma University), and PD20 cells with or without complementation with GFP-hFANCD2 (a gift from Dr Toshiyasu Taniguchi, Fred Hutchinson Cancer Center) were maintained in α-minimum essential medium

(MEM) supplemented with 20% FCS, 1% penicillin and streptomycin. Human ATRIP-GFP-expression vector was transfected into GM6914 and control cells using Lipofectamine LTX according to the manufacturer's instructions. A549 cells expressing ATRIP-GFP have been described (34), and maintained in DMEM with 10% FCS. siRNA transfections were done with Lipofectamine RNAiMAX. The messenger RNA target sequences used for siRNAs were as follows: Rad17 (GAUGGGUCAAC CCAGUCUGTT), TopBP1 (GUGGUUGUAACAGCG CAUC), FANCA (AAGGGUCAAGAGGGAAAA AUA), FANCD2 (CCAUGUCUGCUAAAGAGCGUU CAUU).

Antibodies

Anti-chicken FANCD2 (35) or anti-chicken FANCI (20) serum was described. Other antibodies were purchased from Santa Cruz Biotechnology (polyclonal anti-ATR: sc-1887, polyclonal anti-RAD17: sc-5613, monoclonal anti-Chk1: sc-8408), Bethyl Laboratories (polyclonal anti-FANCA: A301-980A, polyclonal anti-RPA32: A300-244A), Abcam (polyclonal anti-Histone H3: ab1791, polyclonal anti-FANCL: ab42639), Cell Signaling Technology (polyclonal anti-phospho-Chk1-Ser317: #2344), Novus (polyclonal anti-TopBP1: NB100-217, polyclonal human FANCD2: NB100-182, polyclonal anti-FANCG: NBP1-06035), Millipore (monoclonal anti-phospho-ATM-Ser1981: 05–740), Clontech (polyclonal anti-GFP: 632459), Sigma (monoclonal anti-tubulin: T5168) and Upstate Biotechnology (monoclonal anti-CD25: #05–170).

Fractionation of cells and western blotting

Cells were treated with indicated dose of DNA damaging agents and collected. Cell fractionation into soluble and chromatin fractions was done as described previously (36). Briefly, washed cells were resuspended in CSK buffer (10 mM PIPES, pH 7.0, 100 mM NaCl, 300 mM Sucrose, 3 mM $MgCl_2$, 1 mM EGTA, 10 mM NaF, 25 mM β-glycerophosphate, 0.2% Triton X-100, 0.25 mM ATP) containing protease inhibitor tablet (Roche), and centrifuged. Supernatants were saved as soluble fraction. Pellets were further washed using the same buffer twice, and the remained material was used as chromatin fraction. These samples were separated by polyacrylamide gel electrophoreses, transferred to a membrane and detected with indicated antibodies and ECL reagents (GE Healthcare). Phos-tag western blotting was done as described (17). Co-immunoprecipitation assay between overexpressed proteins in 293T cells was carried out as described (27).

Analysis of growth and cell sensitivity toward cisplatin

Cell proliferation rate was assessed as described using plastic microbeads. Cell viability in liquid culture containing cisplatin (Nippon Kayaku, Tokyo, Japan) was assessed after 48 h using FACSCalibur (BD Biosciences) and propidium iodide (PI) staining. Percentage of viable cells was calculated on the basis of forward scatter profile and exclusion of PI fluorescence among the acquired 10 000 events.

Subnuclear focus formation assay

After MMC (Kyowa-Hakkou-Kirin, Tokyo) exposure, cytospin slides or coverslips were fixed with 4% paraformaldehyde/phosphate buffered saline and stained with antibodies against FancD2 or RPA2. Then cells were stained with AlexaFluor-conjugated secondary antibody (Invitrogen) with 4′,6-Diamidino-2-Phenylindole Dihydrochloride (DAPI) counterstaining. Images were captured by fluorescent microscopy (DM5500B, Leica) or confocal laser scanning microscopy (TCS SP5, Leica).

RPA-ssDNA pull-down assay

This assay was carried out essentially as described (37). In brief, biotin-labeled 75 mer ssDNA (5 pmole) was attached to streptavidin-coated magnetic beads (Dynal), and incubated with 400 ng of purified recombinant RPA for 30 min in binding buffer A (10 mM Tris–HCl (pH 7.5), 100 mM NaCl, 10 ng/ml bovine serum albumin (BSA), 0.01% Nonidet P-40, 10% glycerol). The RPA complex was purified as described (38,39) from *Escherichia coli* carrying the RPA-expressing plasmids kindly provided by Dr Marc S. Wold (University of Iowa College of Medicine, Iowa City, Iowa, USA). Cell lines were lysed in 220 μl of lysis buffer (10 mM Tris–HCl (pH 7.5), 100 mM NaCl, 0.05% Nonidet P-40, 10 ng/ml BSA, 10% glycerol). Resultant lysate (100 μl) containing equal amount of protein was then mixed with the beads, and incubated for additional 30 min at room temperature. After washing, the bound material was eluted by addition of sodium dodecyl sulphate-polyacrylamide gel electrophoresis sample buffer and boiling, and examined by western blotting.

Yeast two-hybrid assay

The yeast strain EGY48 (Clontech) was used as a host to express fusion proteins with LexA or B42 transcription activation domain fusion. cDNAs encoding ATRIP, and human FA and FA-related proteins (FANCA, FANCB, FANCC, FANCD2, FANCE, FANCF, FANCG, FANCI, FANCJ, FANCL, FANCM, UBE2T, FAAP24 or FAAP100) were cloned into pLexA (bait) and pB42AD (prey) vectors (Clontech). Sources of the most cDNAs were previously described (17,27,40). FANCM cDNA was provided by Dr Weidong Wang. Human UBE2T or FAAP24 cDNA was amplified from HeLa cell cDNA. The transformants were selected on SD/-Ura/-His/-Trp plate, cultured in liquid of the same medium at 30° for 24 h and then spotted on to SD/-Ura/-His/-Trp/-Leu/+X-gal plates at 30° for 96 h.

RESULTS

Defective localization of ATRIP following MMC damage in cells lacking the FA core complex

At sites of DNA damage and replication fork stress, ATRIP-ATR concentrates in nuclear foci mediated by binding of ATRIP to RPA-coated ssDNA (41). To examine potential interplay between ATR signaling and the FA core complex, we examined focus formation of

ATRIP following MMC-induced DNA damage in FA cells. Available anti-ATRIP antibodies did not allow convincing visualization of focus formation, and so we expressed a human ATRIP-GFP fusion in cells lacking FANCA. In MMC-untreated GFP-positive cells, ATRIP-GFP mostly distributed diffusely throughout the nuclei irrespective of the genotype. On MMC treatment, the complemented control cells displayed robust RPA foci formation that co-localized with ATRIP-GFP foci (Figure 1A). Strikingly, we found that ATRIP-GFP foci in MMC-stimulated FA-A cells were diffuse and greatly reduced, while RPA foci formed normally (Figure 1A). These data suggest that FANCA is required for MMC-induced ATRIP focus formation.

To further study ATRIP localization in the absence of FA proteins, we stably expressed chicken ATRIP-GFP in chicken DT40 WT and FA knockout cell lines. Similar levels of GFP expression among transfectants were confirmed with FACS analysis (Supplementary Figure S1A). Consistent with the results with human FA-A cells, MMC-induced chicken ATRIP-GFP focus formation was abrogated in *fancc* and *fancm* cells (Figure 1B). In contrast, extensive foci formation was still evident in *fancd2* cells, although observed foci were smaller and less intense (Figure 1B). The ATPase activity of the FANCM translocase domain was largely dispensable for focus formation, as shown in cells carrying a D203A knock-in mutation (Figure 1B) (30). The E3 ubiquitin ligase function of FANCL is unlikely to be important for chromatin localization of ATRIP because the E2 enzyme for FANCL, UBE2T, was dispensable for ATRIP focus formation (Figure 1B). The deubiquitinase for FANCD2, USP1, was also not required (Figure 1B). These data suggest that the FA core complex may play an important role in relocalization of ATRIP following DNA damage.

Decreased chromatin localization of ATRIP in cells deficient in the FA core complex

We next determined whether endogenous ATR and ATRIP show defective relocalization to chromatin in human FA cell lines. FA-A (GM6914) and FA-D2 (PD20) cells, with isogenic complemented controls, were treated with MMC, biochemically fractionated and analyzed by western blotting. Consistent with the foci results, FA-A cells displayed a significant reduction (~40%) in MMC-induced chromatin targeting of ATRIP relative to complemented control cells (Figure 2A). ATR localization in GM6914 cells may be deregulated because the ATR level in chromatin was increased in the untreated cells, and was not further increased following MMC treatment. In contrast, MMC-stimulated FA-D2 cells had only minor reduction of ATRIP-ATR levels in chromatin compared with the complemented control cells (Figure 2A). In line with the decreased chromatin binding of ATRIP, phosphorylation of ATRIP on Ser 68 and 72 was decreased to ~50% in FA-A cells but not in FA-D2 cells (Figure 2A and Supplementary Figure S2B and S2C). This phosphorylation event occurs in chromatin and is dependent on ATR (34).

To extend these observations to cells acutely rendered defective in FA proteins, we also examined HeLa S3 cells expressing FLAG-HA-ATRIP treated with siRNAs against FANCA or FANCD2. This cell line expresses ~2-fold more ectopically expressed tagged ATRIP than endogenous ATRIP. Cells depleted of FANCA reduced chromatin ATRIP levels by ~5-fold on MMC damage compared with control cells. The ATR level was also modestly decreased (Figure 2B). This could be partially accounted for by DNA damage-induced decrease in total ATR levels as shown in Figure 2C, though the reduction was greatest in cells exposed to control siRNA. On the other hand, cells depleted of FANCD2 did not have decreased chromatin loading of both ATRIP and ATR (Figure 2B).

Collectively, we conclude that the FA core complex component FANCA promotes or stabilizes chromatin localization of ATRIP in human cells. Combined with the ATRIP-GFP foci results in DT40 cells, the data suggested that the FA core complex as a whole functions to regulate ATRIP levels in chromatin.

The FA core complex is required for ATRIP localization upon replication stress

To address whether the FA core complex plays a similar role following other types of DNA damage, we treated cells with ionizing radiation (IR) or the replication stress inducers MMC, hydroxy Urea (HU) and UV. ATRIP was less phosphorylated on Ser 68/72 in FA-A cells than in isogenic control cells on replication stress, particularly following HU treatment, while the phosphorylation was not decreased in FA-A cells compared with control following IR (Supplementary Figure S3A). Furthermore, the ATRIP-GFP foci formation in *fancc* DT40 cells treated with HU was drastically reduced, while the same cells treated with IR showed similar levels of ATRIP-GFP foci formation to WT cells (Supplementary Figure S3B and S3C). These observations indicate that the dependence of ATRIP localization in chromatin on the FA core complex is dependent on the type of genomic stress. Stalled DNA replication forks (MMC, HU, UV) require the FA core complex for ATRIP localization, but for direct double-strand breaks (IR), FA core complex is not needed.

The FA core complex may physically interact with ATR-ATRIP kinase

Given the above data, we hypothesized that ATRIP may interact with the FA core complex. To test this idea, we carried out yeast two-hybrid interaction assay between ATRIP and various FA and FA-related proteins (including FANCA, FANCB, FANCC, FANCD2, FANCE, FANCF, FANCG, FANCI, FANCJ, FANCL, FANCM, UBE2T, FAAP24 or FAAP100) (Figure 3A). We could detect positive ATRIP interaction only with FANCL or FAAP100.

To determine whether ATRIP could interact with FA core complex components in cells, we co-overexpressed ATRIP with FANCL or FAAP100. Only FANCL co-immunoprecipitated with ATRIP in this setting (Figure 3B). These results suggest that FANCL might be the core complex subunit that associates with ATRIP protein.

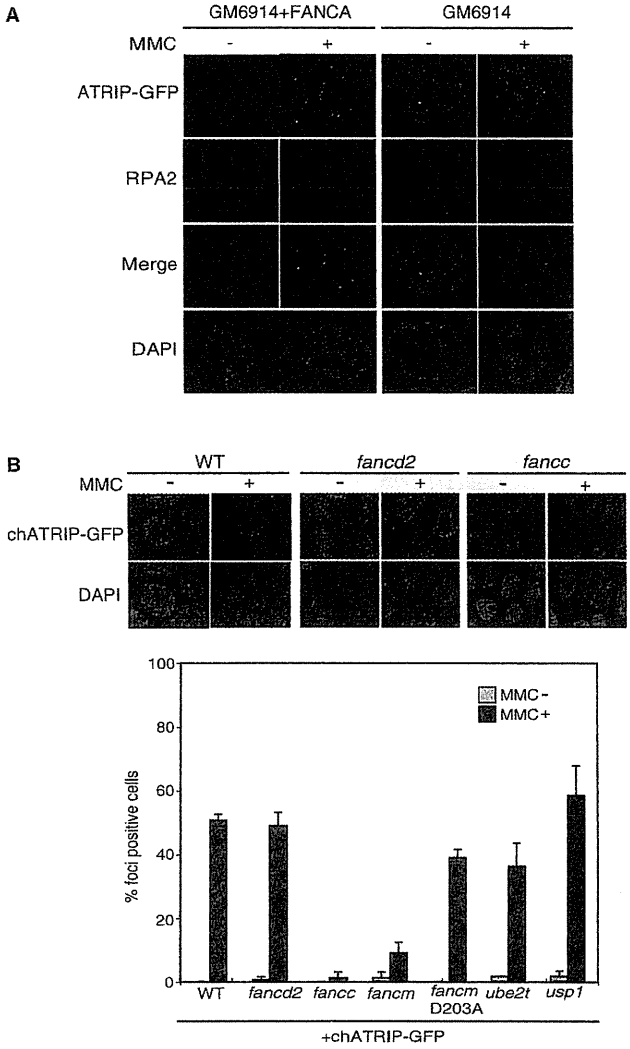

Figure 1. Defective ATRIP-GFP foci formation in FA cells. (**A**) MMC-induced human ATRIP-GFP foci formation in human FA-A (GM6914) and complemented control cells. Following transient transfection of the ATRIP-GFP expression vector, ~10% of the cells became GFP-positive 24 h after transfection. Then the cells were treated with or without MMC (100 ng/ml for 24 h), fixed and stained with anti-RPA2 antibody, and the GFP was visualized directly. The images were captured by confocal laser scanning microscopy. (**B**) MMC-induced chicken ATRIP-GFP foci in chicken DT40 mutant cells. Indicated DT40 WT and FA mutant cells were stably transfected with chicken ATRIP-GFP expression vector. Clones selected on the basis of similar GFP expression levels were subjected to analysis. Following MMC treatment (500 ng/ml for 6 h), cells were fixed, and observed by confocal laser scanning microscopy. The bar graph represents mean and SD of % GFP-foci positive cells in three independent experiments. Fifty nuclei were scored in each case, and nuclei containing more than four bright GFP foci were defined as foci positive.

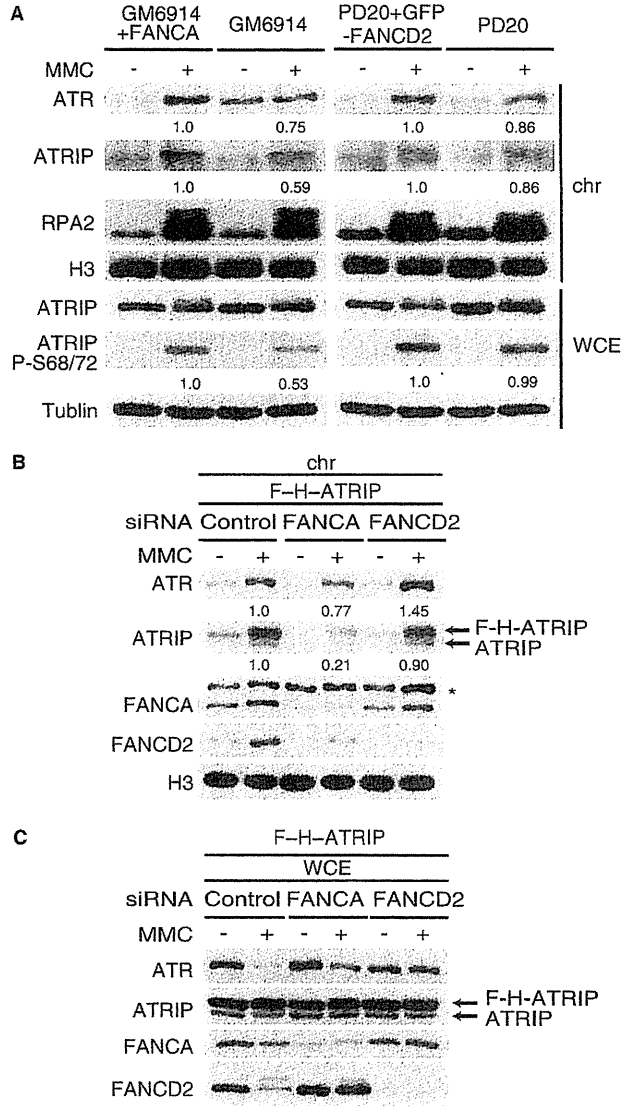

Figure 2. Chromatin localization of ATRIP is defective in human cells lacking the FA core complex. (**A**) FA-A (GM6914 fibroblast) or FA-D2 (PD20 fibroblast) and respective complemented control cells were treated with MMC (100 ng/ml for 24 h). The whole cell extract (WCE) and the chromatin fraction (chr) were prepared and analyzed by western blotting. (**B** and **C**) HeLa S3 cells expressing FLAG-HA-ATRIP (F-H-ATRIP) were transfected with siRNAs targeting FANCA or FANCD2. After 48 h, the cells were stimulated with MMC (100 ng/ml for 24 h). Chromatin fraction (B) or WCE (C) were analyzed by western blotting. The numbers indicate the ratio of the band intensity normalized to the control lane.

The FA core complex promotes binding of ATRIP to RPA-coated ssDNA

To gain further insight into the role of the core complex in the ATRIP recruitment to RPA-coated ssDNA, we assessed the amount of ATRIP protein that could be recovered from cell extracts following binding to RPA-coated ssDNA (Figure 3C). In the extracts lacking the core complex, significantly less ATRIP protein was pulled down compared with the matched control cell extracts (indicated as +A). Interestingly, the core complex components such as FANCA could be recovered from control cell extract by ssDNA beads without exogenous RPA complex. These data suggest that the core complex bound to RPA-coated ssDNA may facilitate or

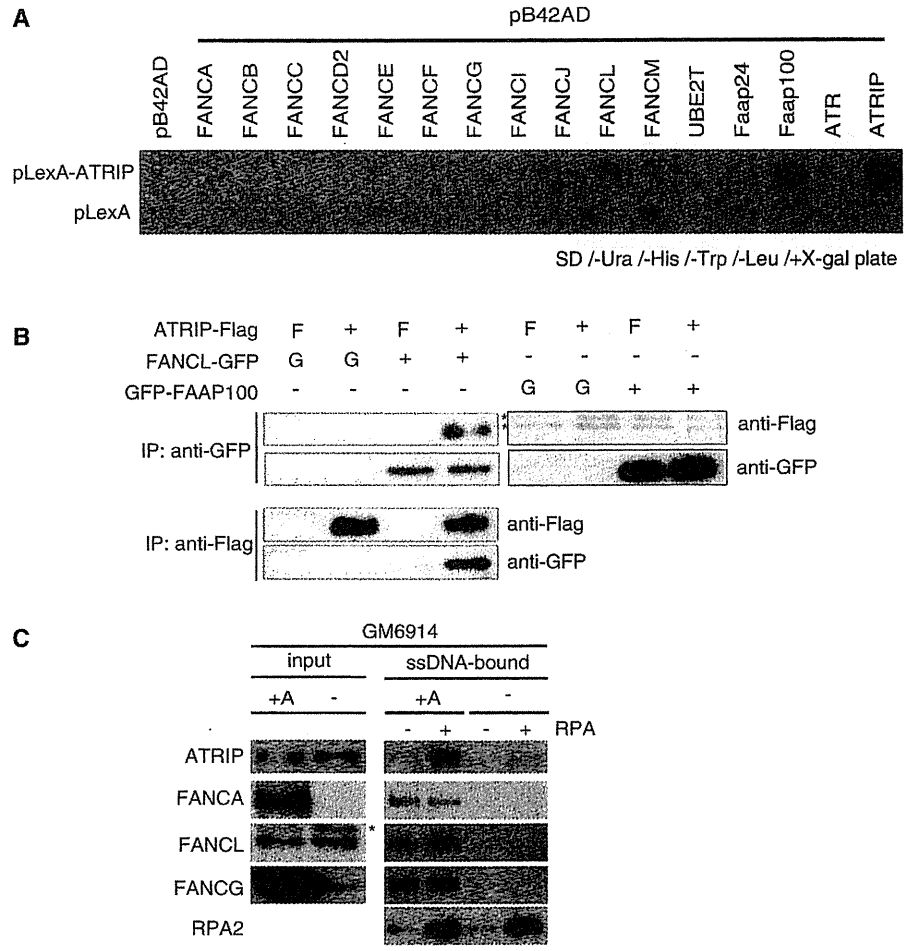

Figure 3. Interplay between FA proteins and ATRIP. (**A**) Yeast two-hybrid interaction assay between ATRIP and various full-length FA or FA-related proteins. Selected yeast transformants were spotted onto SD/-Ura/-His/-Trp/-Leu/+X-gal plates at 30° for 96 h. ATRIP–ATRIP interaction served as positive control. (**B**) Co-immunoprecipitation assay between overexpressed human FANCL-GFP or GFP-FAAP100 and ATRIP-Flag in 293T cells. F or G, Flag or GFP vector without insert. (**C**) RPA-ssDNA pull-down assay from extracts of FA-A (GM6914) and complemented FA-A cells (+A). ssDNA-attached magnetic beads preincubated with or without recombinant RPA were mixed with cell extracts. After washing, the bound material was analyzed by western blotting.

stabilize ATRIP binding to RPA through either direct or indirect interaction with ATRIP.

Loss of FANCI phosphorylation in cells lacking the FA core components

We wished to determine how the deficiency in the FA core complex affects signaling events through ATR because the altered ATRIP-ATR chromatin localization should have a consequence on downstream signaling events. Although mild S-phase checkpoint defects in FA cell lines have been reported (42–44), MMC-induced CHK1 phosphorylation was not significantly affected in cells deficient in the FA core components (Figure 4A, C and D). Interestingly, previous reports have indicated that CHK1 phosphorylation can occur without ATRIP focus formation, in cells harboring an ATRIP N-terminal deletion (45,46) or an LG mutant (47), which is incapable of binding to RPA or is deficient in dimerization (37,48). Further, stimulation of ATR activity by TOPBP1 can occur in the absence of RPA binding to ATRIP (49). Thus, an association of a residual amount of ATRIP-ATR kinase with TOPBP1 in chromatin might be sufficient to phosphorylate CHK1.

Next, we investigated FANCI phosphorylation in DT40 mutants because FANCI is the critical ATR substrate in the FA pathway (20) following DNA damage. We used the Phos-tag western blotting (17) to detect phosphorylated FANCI. Phospho-proteins could be detected as slower migrating bands in a Phos-tag-containing polyacrylamide gel electrophoresis gel. *FANCI* K525R knock-in DT40 cells were used as a control, in which the FANCI monoubiquitination site (Lysine) was replaced with Arginine by gene targeting (Supplementary Figure S4). This mutant was defective in FANCI monoubiquitination, similarly to *fancl, fancc* and *fancd2* mutants, yet FANCI phosphorylation was clearly observed (Figure 4B).

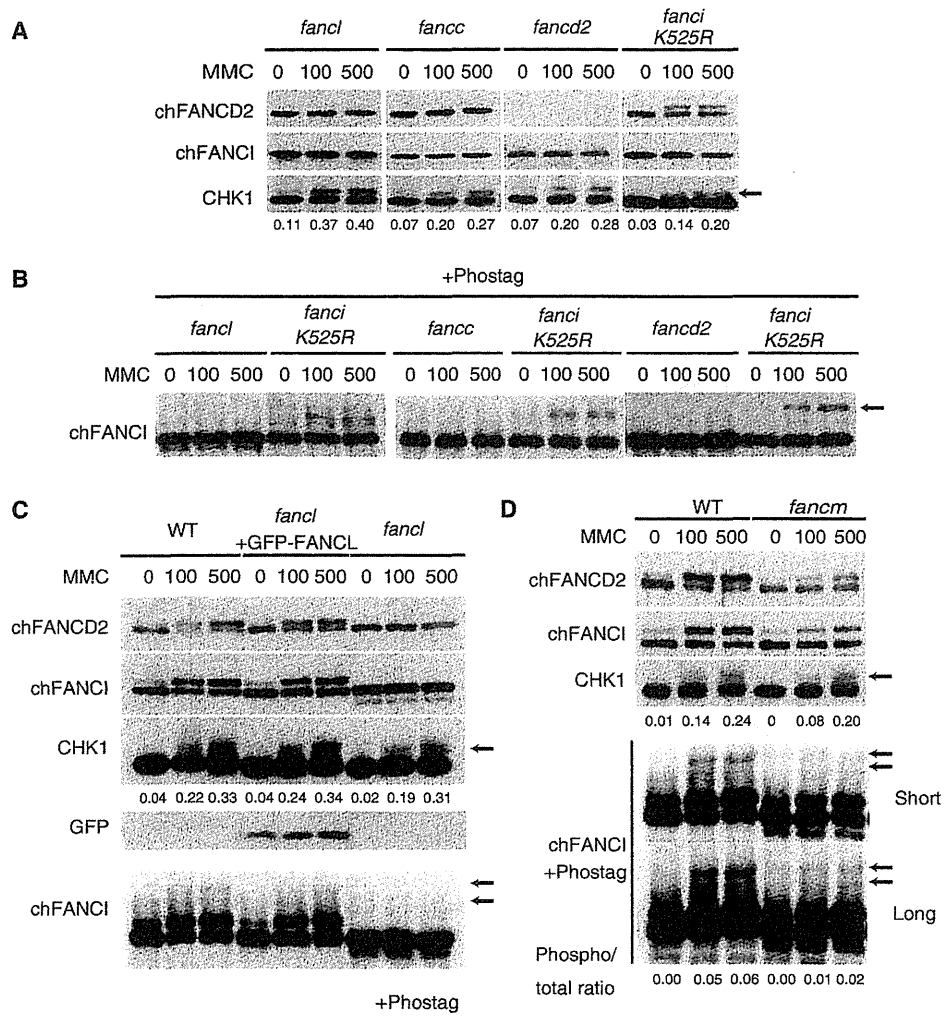

Figure 4. FANCI phosphorylation mediated by ATR is defective in cells lacking FANCD2 or the FA core complex. (**A**) Cells were treated with MMC (100 or 500 ng/ml for 6 h) and analyzed with western blotting. (**B**) Samples were prepared as in A, and analyzed with Phos-tag western blotting. (**C**) Phos-tag western blotting of FancI protein in *fancl* cells and cells complemented with GFP-chFANCL. (**D**) WT and *fancm* cells were stimulated as indicated and analyzed by western blotting with or without Phos-tag. Numbers indicate ratio of phosphorylated CHK1 or FANCI to total CHK1 or FANCI, respectively.

Strikingly, *fancl, fancc* and *fancd2* mutant cells were completely deficient in FANCI phosphorylation (Figure 4B). Furthermore, *fancl* cells complemented with GFP-chFANCL (27) could phosphorylate FANCI at a level comparable with WT cells (Figure 4C). *fancm* cells showed an intermediate phenotype, with FANCI phosphorylation ~20–30% of normal observed following MMC treatment (Figure 4D). This is consistent with the weakened but still clearly detectable FANCD2 monoubiquitination in *fancm* cells (Figure 4D). A stimulatory role of *FANCM* in FANCD2 monoubiquitination has been previously described (29,50–52).

FA pathway activation is independent of RAD17 or TOPBP1

The results described above and our previous studies (17,20) clearly indicated that FANCI phosphorylation is mediated by ATR kinase in a manner dependent on the FA core complex and FANCD2 protein. This phosphorylation event then triggers FA pathway activation, leading to FANCD2 monoubiquitination and DNA repair. It has been well accepted that the phosphorylation of the ATR substrates requires the kinase activator TOPBP1 as well as its recruiter, the 9-1-1 complex, which is loaded by the RAD17-RFC complex (21–23). To gain more insight into the interplay between ATR and the FA pathway, we wished to test whether the activation of the FA pathway is affected by the absence of the canonical ATR activators RAD17 or TOPBP1. Surprisingly, MMC-induced FANCD2 and FANCI monoubiquitination were only slightly affected by the loss of RAD17 gene (Figure 5A), while CHK1 phosphorylation was severely diminished in the knockout DT40 cell lines (Figure 5A). Consistently, FANCI phosphorylation was

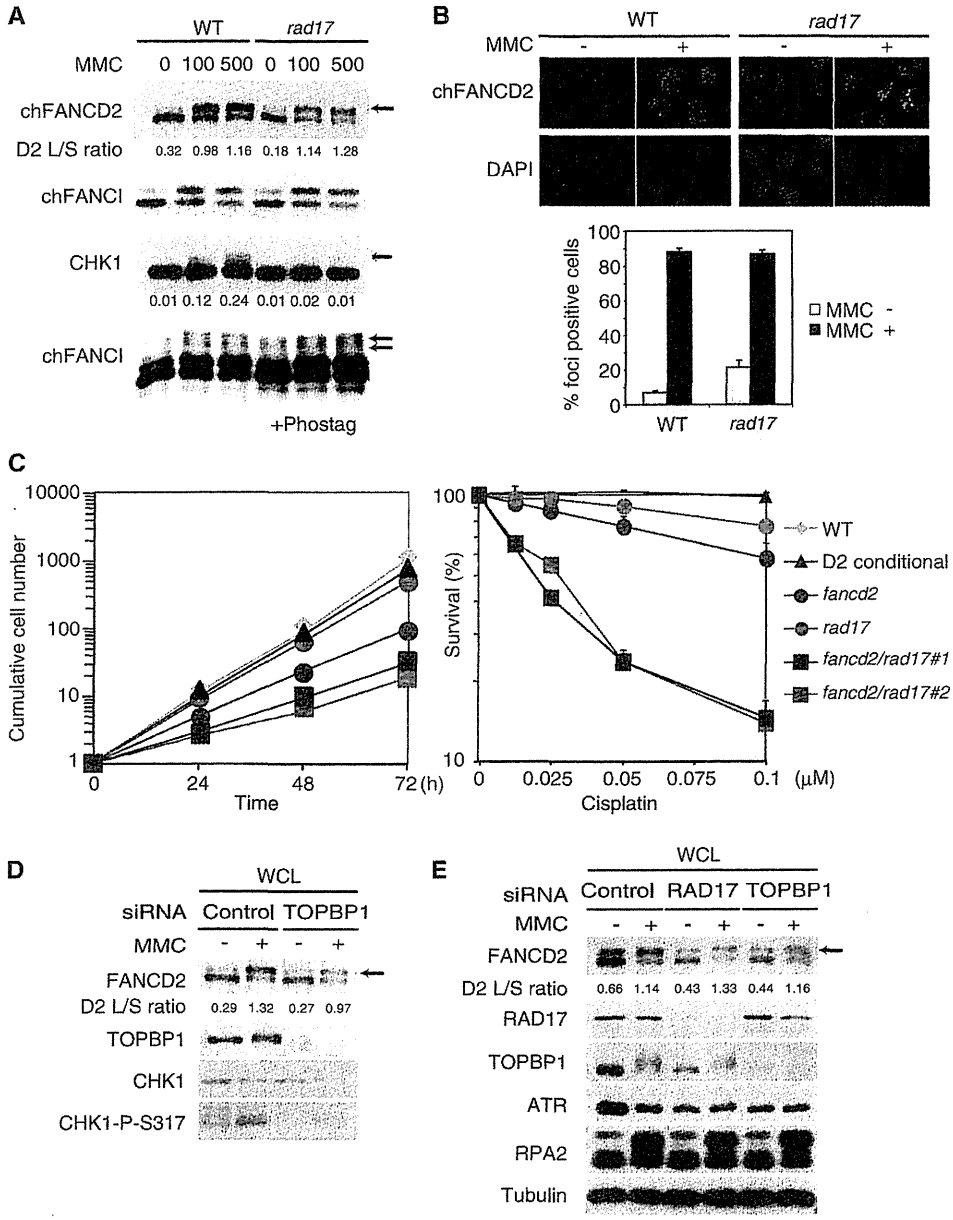

Figure 5. RAD17 and TOPBP1 are dispensable for FA pathway activation. (**A**) Cells were treated with MMC (100 or 500 ng/ml for 6 h) and analyzed with western blotting with or without Phos-tag. Numbers indicate ratio of phosphorylated CHK1 to total CHK1. (**B**) FANCD2 foci formation following MMC treatment (500 ng/ml for 6 h) was analyzed in DT40 WT and *rad17* mutant cells by fluorescent microscopy. The bar graph represents mean and SD of % FANCD2-foci positive cells in three independent experiments. Fifty nuclei were scored in each case, and nuclei containing more than four bright foci were defined as foci positive. (**C**) Cell growth rate (left panel) and % survival of the cells cultured for 48 h in the medium containing cisplatin (right panel). Cell number or cell viability was assessed by flow cytometry using plastic microbeads or PI staining, respectively. The error bar represents SD in three independent experiments. (**D** and **E**) HeLa S3 cells (D) or A549 cells expressing ATRIP-GFP (E) were transfected with indicated siRNAs. After 48 h, cells were treated with MMC (100 ng/ml) for additional 24 h. WCE was analyzed by western blotting.

not defective in *rad17* cells (Figure 5A). FANCD2 focus formation was also not affected (Figure 5B). These data indicate that the FA pathway activation occurs independently of RAD17.

To verify this conclusion by a genetic test, we generated a double knockout DT40 cell line lacking both *RAD17* and *FANCD2* genes (Supplementary Figure S5). The double knockout cells grew slower and were much more sensitive to cisplatin compared with either single mutant cell line (Figure 5C), suggesting a synergistic relationship. We also used siRNA knockdown in HeLa S3 or A549 cells expressing ATRIP-GFP. FANCD2 monoubiquitination

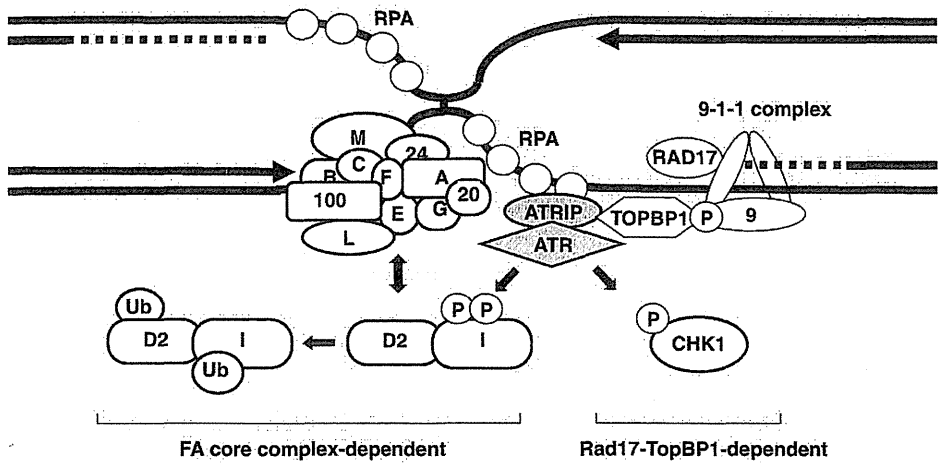

Figure 6. Our proposed model for two distinct pathways in ICL-induced ATR signaling. RPA complex accumulates on exposed ssDNA region surrounding the ICL (middle). RPA-ATRIP binding, which is facilitated by the FA core complex, promotes ATR recruitment. In the left side of the pathway, which is dependent on the FA core complex but not on the RAD17-TOPBP1 pathway, FANCI is phosphorylated, triggering FANCD2 monoubiquitination. In the right side, CHK1 is phosphorylated depending on the RAD17-TOPBP1 pathway, but the FA core complex is largely dispensable for the CHK1 activation.

was affected only slightly by siTOPBP1 treatment in HeLa S3 (L/S ratio 1.32 in control versus 0.97 in TOPBP1-depleted cells), whereas CHK1 phosphorylation was mostly abrogated (Figure 5D). In siRAD17- or siTOPBP1-treated A549 cells (Figure 5E), FANCD2 monoubiquitination was only slightly diminished compared with control. Furthermore, FANCD2 still efficiently accumulated in subnuclear foci and in chromatin following MMC damage similarly to cells transfected with control siRNA (Supplementary Figure S6A and B).

DISCUSSION

ATRIP-ATR kinase is essential for checkpoint signaling via CHK1 phosphorylation (21–23), and it is also required for DNA repair by activating the FA pathway through FANCI phosphorylation (17,20). It has been well accepted that ATR signaling proceeds in two steps: a localization step via ATRIP-RPA interaction, and then enzymatic activation by ATR-TOPBP1 interaction. In this study, we attempted to clarify interplay between ATR signaling and the FA pathway. Our data indicate that the FA core complex (including FANCM) regulates the former step, and also connects ATR and the FA pathway activation. On the other hand, the latter step is not critical for the FA pathway. There have been several reports that demonstrate roles of the FANCM/FAAP24 complex in the ATR signaling independent of the FA core complex (52–56). For example, FANCM has a role for chromatin accumulation of RPA (55,56) or TOPBP1 (54) following DNA damage. Our results complement these previous studies and indicate that other components of the FA core complex have a role in the ATR signaling.

In the current study, we provide evidence that the FA core complex affects the localization step by facilitating ATRIP interaction with RPA-ssDNA. Of note, FANCL has been reported to play an upstream role in RPA-ATR-Chk1 signaling in Xenopus egg extracts stimulated by plasmids carrying an ICL (57). The present results extend these studies to deletion of specific components of the FA core complex in mammalian and avian somatic cells, and reveal that FA core complex defects are associated with impaired intracellular and chromatin localization of ATRIP.

The mechanisms for enhancing ATRIP-RPA interaction remain unknown. ATRIP-FANCL interaction was detected using yeast two-hybrid assay and by co-immunoprecipitation of the transfected proteins. However, whether the endogenous proteins actually interact is currently unclear. Because the E2 enzyme UBE2T is not required for this process, the FA core complex stabilizes the interaction independently of the ubiquitination activity. The ATPase activity of FANCM is also dispensable. A previous study indicated that *in vitro* binding of ATRIP-ATR to RPA-ssDNA is enhanced by an unknown human protein (37). It will be interesting to test whether this unknown factor is a component of the FA core complex.

We showed that, in cells lacking the FA core complex, phosphorylation of ATRIP as well as FANCI protein is defective. MMC-induced CHK1 phosphorylation occurs normally in FA knockout cells. Loss of FANCI phosphorylation is functionally important because it is the triggering event in activation of the FA pathway (17). However, it is obscure whether defective ATRIP-ATR chromatin localization is the direct cause of the loss of FANCI phosphorylation. The FA core complex may function

downstream of ATRIP-ATR as an essential link to connect FANCI with ATR, resulting in FANCI phosphorylation. It is possible that ATR phosphorylates FANCI when it is in a complex with FANCD2. We have previously reported that efficiency of FANCI phosphorylation by ATR *in vitro* is enhanced by the presence of FANCD2 (20). Interestingly, a recent report suggests that chromatin binding of FANCI depends on FANCD2 in Xenopus egg extracts (58). Collectively, these results indicate the defective core complex abolishes the upstream phosphorylation events on FANCI in addition to its ubiquitin E3 ligase activity, thus blocking the FA pathway signaling at two levels.

Our data also indicate that TOPBP1 and RAD17 do not play a major role in FA pathway activation. This is consistent with our previous observation that ATRIP does not require TOPBP1 interaction to activate the FA pathway (20). An *in vitro* study has shown that at high concentration of substrate the influence of TOPBP1 on ATR kinase activity is less pronounced (59). In FA pathway activation, the phosphorylation substrate FANCI may accumulate in damaged chromatin, perhaps though the interaction with FANCD2 and/or the core complex (60,61), achieving concentrations that reduce the requirement for TOPBP1. Alternatively, the locally accumulated ATRIP-ATR might have sufficient activity to phosphorylate FANCI without TOPBP1 stimulation. Interestingly, auto-phosphorylation of ATR on Thr 1989 is not dependent on the presence of TOPBP1 (62).

Given these findings, we propose two distinct subpathways in ATR signaling (Figure 6). One is dependent on RAD17-TOPBP1 pathway in which the important substrate is CHK1. This pathway is also affected by the FANCM-FAAP24 subcomplex. The other pathway is dependent on the FA core complex, and critical for phosphorylating ATRIP, FANCI and perhaps FANCD2 and BLM (63). Other substrates in this subpathway of ATR signaling may be identified.

SUPPLEMENTARY DATA

Supplementary Data are available at NAR Online: Supplementary Figures 1–6.

ACKNOWLEDGEMENTS

The authors thank Drs Richard D. Wood (MD Anderson Cancer Center) and Agata Smogorzewska (Rockefeller University) for critical reading of the manuscript; Drs Kyoji Horie, Toshiyasu Taniguchi, K.J. Patel, Weidong Wang, Marc S. Wold, Takayuki Yamashita for reagents; Drs Hitoshi Kurumizaka and Hiroshi Kimura for FANCD2 siRNA sequence; Drs Kenshi Komatsu, Junya Kobayashi, Nigel Jones for advice and help; Ms Seiko Arai for secretarial assistance.

FUNDING

Ministry of Education, Science, Sports and Culture of Japan [JSPS KAKENHI, 21390094 and MEXT KAKENHI, 23114010] (in part); The Uehara Memorial Foundation (to M.T.); Takeda foundation (to M.T.); the Ichiro Kanehara Foundation (to M.I.); the Mochida Memorial Foundation for Medical and Pharmaceutical Research (to M.I.). Funding for open access charge: Grants-in aid from the Ministry of Education, Science, Sports and Culture of Japan.

Conflict of interest statement. None declared.

REFERENCES

1. Kim,H. and D'Andrea,A.D. (2012) Regulation of DNA cross-link repair by the Fanconi anemia/BRCA pathway. *Genes Dev.*, **26**, 1393–1408.
2. Wang,W. (2007) Emergence of a DNA-damage response network consisting of Fanconi anaemia and BRCA proteins. *Nat. Rev. Genet.*, **8**, 735–748.
3. Kim,J.M., Kee,Y., Gurtan,A. and D'Andrea,A.D. (2008) Cell cycle-dependent chromatin loading of the Fanconi anemia core complex by FANCM/FAAP24. *Blood*, **111**, 5215–5222.
4. Ciccia,A., Ling,C., Coulthard,R., Yan,Z., Xue,Y., Meetei,A.R., Laghmani el,H., Joenje,H., McDonald,N., de Winter,J.P. *et al.* (2007) Identification of FAAP24, a Fanconi anemia core complex protein that interacts with FANCM. *Mol. Cell*, **25**, 331–343.
5. Kee,Y. and D'Andrea,A.D. (2010) Expanded roles of the Fanconi anemia pathway in preserving genomic stability. *Genes Dev.*, **24**, 1680–1694.
6. Smogorzewska,A., Matsuoka,S., Vinciguerra,P., McDonald,E.R. 3rd, Hurov,K.E., Luo,J., Ballif,B.A., Gygi,S.P., Hofmann,K., D'Andrea,A.D. *et al.* (2007) Identification of the FANCI protein, a monoubiquitinated FANCD2 paralog required for DNA repair. *Cell*, **129**, 289–301.
7. Huang,M. and D'Andrea,A.D. (2010) A new nuclease member of the FAN club. *Nat. Struct. Mol. Biol.*, **17**, 926–928.
8. Sato,K., Ishiai,M., Toda,K., Furukoshi,S., Osakabe,A., Tachiwana,H., Takizawa,Y., Kagawa,W., Kitao,H., Dohmae,N. *et al.* (2012) Histone chaperone activity of Fanconi anemia proteins, FANCD2 and FANCI, is required for DNA crosslink repair. *EMBO J.*, **31**, 3524–3536.
9. Matsushita,N., Kitao,H., Ishiai,M., Nagashima,N., Hirano,S., Okawa,K., Ohta,T., Yu,D.S., McHugh,P.J., Hickson,I.D. *et al.* (2005) A FancD2-monoubiquitin fusion reveals hidden functions of Fanconi anemia core complex in DNA repair. *Mol. Cell*, **19**, 841–847.
10. Walsh,T. and King,M.C. (2007) Ten genes for inherited breast cancer. *Cancer Cell*, **11**, 103–105.
11. Levy-Lahad,E. (2010) Fanconi anemia and breast cancer susceptibility meet again. *Nat. Genet.*, **42**, 368–369.
12. Vaz,F., Hanenberg,H., Schuster,B., Barker,K., Wiek,C., Erven,V., Neveling,K., Endt,D., Kesterton,I., Autore,F. *et al.* (2010) Mutation of the RAD51C gene in a Fanconi anemia-like disorder. *Nat. Genet.*, **42**, 406–409.
13. Stoepker,C., Hain,K., Schuster,B., Hilhorst-Hofstee,Y., Rooimans,M.A., Steltenpool,J., Oostra,A.B., Eirich,K., Korthof,E.T., Nieuwint,A.W. *et al.* (2011) SLX4, a coordinator of structure-specific endonucleases, is mutated in a new Fanconi anemia subtype. *Nat. Genet.*, **43**, 138–141.
14. Kim,Y., Lach,F.P., Desetty,R., Hanenberg,H., Auerbach,A.D. and Smogorzewska,A. (2011) Mutations of the SLX4 gene in Fanconi anemia. *Nat. Genet.*, **43**, 142–146.
15. Yamamoto,K.N., Kobayashi,S., Tsuda,M., Kurumizaka,H., Takata,M., Kono,K., Jiricny,J., Takeda,S. and Hirota,K. (2011) Involvement of SLX4 in interstrand cross-link repair is regulated by the Fanconi anemia pathway. *Proc. Natl Acad. Sci. USA*, **108**, 6492–6496.
16. Crossan,G.P., van der Weyden,L., Rosado,I.V., Langevin,F., Gaillard,P.H., McIntyre,R.E., Gallagher,F., Kettunen,M.I., Lewis,D.Y., Brindle,K. *et al.* (2011) Disruption of mouse Slx4, a regulator of structure-specific nucleases, phenocopies Fanconi anemia. *Nat. Genet.*, **43**, 147–152.

17. Ishiai,M., Kitao,H., Smogorzewska,A., Tomida,J., Kinomura,A., Uchida,E., Saberi,A., Kinoshita,E., Kinoshita-Kikuta,E., Koike,T. *et al.* (2008) FANCI phosphorylation functions as a molecular switch to turn on the Fanconi anemia pathway. *Nat. Struct. Mol. Biol.*, **15**, 1138–1146.
18. Andreassen,P.R., D'Andrea,A.D. and Taniguchi,T. (2004) ATR couples FANCD2 monoubiquitination to the DNA-damage response. *Genes Dev.*, **18**, 1958–1963.
19. Wang,L.C., Stone,S., Hoatlin,M.E. and Gautier,J. (2008) Fanconi anemia proteins stabilize replication forks. *DNA Repair (Amst.)*, **7**, 1973–1981.
20. Shigechi,T., Tomida,J., Sato,K., Kobayashi,M., Eykelenboom,J.K., Pessina,F., Zhang,Y., Uchida,E., Ishiai,M., Lowndes,N.F. *et al.* (2012) ATR-ATRIP kinase complex triggers activation of the Fanconi anemia DNA repair pathway. *Cancer Res.*, **72**, 1149–1156.
21. Cimprich,K.A. and Cortez,D. (2008) ATR: an essential regulator of genome integrity. *Nat. Rev. Mol. Cell Biol.*, **9**, 616–627.
22. Burrows,A.E. and Elledge,S.J. (2008) How ATR turns on: TopBP1 goes on ATRIP with ATR. *Genes Dev.*, **22**, 1416–1421.
23. Flynn,R.L. and Zou,L. (2010) ATR: a master conductor of cellular responses to DNA replication stress. *Trends Biochem. Sci.*, **36**, 133–140.
24. Takao,N., Kato,H., Mori,R., Morrison,C., Sonada,E., Sun,X., Shimizu,H., Yoshioka,K., Takeda,S. and Yamamoto,K. (1999) Disruption of ATM in p53-null cells causes multiple functional abnormalities in cellular response to ionizing radiation. *Oncogene*, **18**, 7002–7009.
25. Kobayashi,M., Hirano,A., Kumano,T., Xiang,S.L., Mihara,K., Haseda,Y., Matsui,O., Shimizu,H. and Yamamoto,K. (2004) Critical role for chicken Rad17 and Rad9 in the cellular response to DNA damage and stalled DNA replication. *Genes Cells*, **9**, 291–303.
26. Hirano,S., Yamamoto,K., Ishiai,M., Yamazoe,M., Seki,M., Matsushita,N., Ohzeki,M., Yamashita,Y.M., Arakawa,H., Buerstedde,J.M. *et al.* (2005) Functional relationships of FANCC to homologous recombination, translesion synthesis, and BLM. *EMBO J.*, **24**, 418–427.
27. Seki,S., Ohzeki,M., Uchida,A., Hirano,S., Matsushita,N., Kitao,H., Oda,T., Yamashita,T., Kashihara,N., Tsubahara,A. *et al.* (2007) A requirement of FancL and FancD2 monoubiquitination in DNA repair. *Genes Cell*, **12**, 299–310.
28. Yamamoto,K., Hirano,S., Ishiai,M., Morishima,K., Kitao,H., Namikoshi,K., Kimura,M., Matsushita,N., Arakawa,H., Buerstedde,J.M. *et al.* (2005) Fanconi anemia protein FANCD2 promotes immunoglobulin gene conversion and DNA repair through a mechanism related to homologous recombination. *Mol. Cell. Biol.*, **25**, 34–43.
29. Mosedale,G., Niedzwiedz,W., Alpi,A., Perrina,F., Pereira-Leal,J.B., Johnson,M., Langevin,F., Pace,P. and Patel,K.J. (2005) The vertebrate Hef ortholog is a component of the Fanconi anemia tumor-suppressor pathway. *Nat. Struct. Mol. Biol.*, **12**, 763–771.
30. Rosado,I.V., Niedzwiedz,W., Alpi,A.F. and Patel,K.J. (2009) The Walker B motif in avian FANCM is required to limit sister chromatid exchanges but is dispensable for DNA crosslink repair. *Nucleic Acids Res.*, **37**, 4360–4370.
31. Oestergaard,V.H., Langevin,F., Kuiken,H.J., Pace,P., Niedzwiedz,W., Simpson,L.J., Ohzeki,M., Takata,M., Sale,J.E. and Patel,K.J. (2007) Deubiquitination of FANCD2 is required for DNA crosslink repair. *Mol. Cell*, **28**, 798–809.
32. Alpi,A., Langevin,F., Mosedale,G., Machida,Y.J., Dutta,A. and Patel,K.J. (2007) UBE2T, the Fanconi anemia core complex, and FANCD2 are recruited independently to chromatin: a basis for the regulation of FANCD2 monoubiquitination. *Mol. Cell. Biol.*, **27**, 8421–8430.
33. Ikura,T., Ogryzko,V.V., Grigoriev,M., Groisman,R., Wang,J., Horikoshi,M., Scully,R., Qin,J. and Nakatani,Y. (2000) Involvement of the TIP60 histone acetylase complex in DNA repair and apoptosis. *Cell*, **102**, 463–473.
34. Itakura,E., Umeda,K., Sekoguchi,E., Takata,H., Ohsumi,M. and Matsuura,A. (2004) ATR-dependent phosphorylation of ATRIP in response to genotoxic stress. *Biochem. Biophys. Res. Commun.*, **323**, 1197–1202.
35. Yoshikiyo,K., Kratz,K., Hirota,K., Nishihara,K., Takata,M., Kurumizaka,H., Horimoto,S., Takeda,S. and Jiricny,J. (2010) KIAA1018/FAN1 nuclease protects cells against genomic instability induced by interstrand cross-linking agents. *Proc. Natl Acad. Sci. USA*, **107**, 21553–21557.
36. Liu,P., Barkley,L.R., Day,T., Bi,X., Slater,D.M., Alexandrow,M.G., Nasheuer,H.P. and Vaziri,C. (2006) The Chk1-mediated S-phase checkpoint targets initiation factor Cdc45 via a Cdc25A/Cdk2-independent mechanism. *J. Biol. Chem.*, **281**, 30631–30644.
37. Namiki,Y. and Zou,L. (2006) ATRIP associates with replication protein A-coated ssDNA through multiple interactions. *Proc. Natl Acad. Sci. USA*, **103**, 580–585.
38. Henricksen,L.A., Umbricht,C.B. and Wold,M.S. (1994) Recombinant replication protein A: expression, complex formation, and functional characterization. *J. Biol. Chem.*, **269**, 11121–11132.
39. Masuda,Y., Suzuki,M., Piao,J., Gu,Y., Tsurimoto,T. and Kamiya,K. (2007) Dynamics of human replication factors in the elongation phase of DNA replication. *Nucleic Acids Res.*, **35**, 6904–6916.
40. Sato,K., Toda,K., Ishiai,M., Takata,M. and Kurumizaka,H. (2012) DNA robustly stimulates FANCD2 monoubiquitylation in the complex with FANCI. *Nucleic Acids Res.*, **40**, 4553–4561.
41. Zou,L. and Elledge,S.J. (2003) Sensing DNA damage through ATRIP recognition of RPA-ssDNA complexes. *Science*, **300**, 1542–1548.
42. Sala-Trepat,M., Rouillard,D., Escarceller,M., Laquerbe,A., Moustacchi,E. and Papadopoulo,D. (2000) Arrest of S-phase progression is impaired in Fanconi anemia cells. *Exp. Cell Res.*, **260**, 208–215.
43. Centurion,S.A., Kuo,H.R. and Lambert,W.C. (2000) Damage-resistant DNA synthesis in Fanconi anemia cells treated with a DNA cross-linking agent. *Exp. Cell Res.*, **260**, 216–221.
44. Pichierri,P. and Rosselli,F. (2004) The DNA crosslink-induced S-phase checkpoint depends on ATR-CHK1 and ATR-NBS1-FANCD2 pathways. *EMBO J.*, **23**, 1178–1187.
45. Ball,H.L., Myers,J.S. and Cortez,D. (2005) ATRIP binding to replication protein A-single-stranded DNA promotes ATR-ATRIP localization but is dispensable for Chk1 phosphorylation. *Mol. Biol. Cell*, **16**, 2372–2381.
46. Itakura,E., Takai,K.K., Umeda,K., Kimura,M., Ohsumi,M., Tamai,K. and Matsuura,A. (2004) Amino-terminal domain of ATRIP contributes to intranuclear relocation of the ATR-ATRIP complex following DNA damage. *FEBS Lett.*, **577**, 289–293.
47. Itakura,E., Sawada,I. and Matsuura,A. (2005) Dimerization of the ATRIP protein through the coiled-coil motif and its implication to the maintenance of stalled replication forks. *Mol. Biol. Cell*, **16**, 5551–5562.
48. Ball,H.L. and Cortez,D. (2005) ATRIP oligomerization is required for ATR-dependent checkpoint signaling. *J. Biol. Chem.*, **280**, 31390–31396.
49. Ball,H.L., Ehrhardt,M.R., Mordes,D.A., Glick,G.G., Chazin,W.J. and Cortez,D. (2007) Function of a conserved checkpoint recruitment domain in ATRIP proteins. *Mol. Cell. Biol.*, **27**, 3367–3377.
50. Bakker,S.T., van de Vrugt,H.J., Rooimans,M.A., Oostra,A.B., Steltenpool,J., Delzenne-Goette,E., van der Wal,A., van der Valk,M., Joenje,H., te Riele,H. *et al.* (2009) Fancm-deficient mice reveal unique features of Fanconi anemia complementation group M. *Hum. Mol. Genet.*, **18**, 3484–3495.
51. Singh,T.R., Bakker,S.T., Agarwal,S., Jansen,M., Grassman,E., Godthelp,B.C., Ali,A.M., Du,C.H., Rooimans,M.A., Fan,Q. *et al.* (2009) Impaired FANCD2 monoubiquitination and hypersensitivity to camptothecin uniquely characterize Fanconi anemia complementation group M. *Blood*, **114**, 174–180.
52. Wang,Y., Leung,J.W., Jiang,Y., Lowery,M.G., Do,H., Vasquez,K.M., Chen,J., Wang,W. and Li,L. (2013) FANCM and FAAP24 Maintain Genome Stability via Cooperative as Well as Unique Functions. *Mol. Cell*, **49**, 997–1009.
53. Collis,S.J., Ciccia,A., Deans,A.J., Horejsi,Z., Martin,J.S., Maslen,S.L., Skehel,J.M., Elledge,S.J., West,S.C. and Boulton,S.J. (2008) FANCM and FAAP24 function in ATR-mediated

checkpoint signaling independently of the fanconi anemia core complex. *Mol. Cell*, **32**, 313–324.
54. Schwab,R.A., Blackford,A.N. and Niedzwiedz,W. (2010) ATR activation and replication fork restart are defective in FANCM-deficient cells. *EMBO J.*, **29**, 806–818.
55. Huang,M., Kim,J.M., Shiotani,B., Yang,K., Zou,L. and D'Andrea,A.D. (2010) The FANCM/FAAP24 complex is required for the DNA interstrand crosslink-induced checkpoint response. *Mol. Cell*, **39**, 259–268.
56. Duquette,M.L., Zhu,Q., Taylor,E.R., Tsay,A.J., Shi,L.Z., Berns,M.W. and McGowan,C.H. (2012) CtIP is required to initiate replication-dependent interstrand crosslink repair. *PLoS Genet.*, **8**, e1003050.
57. Ben-Yehoyada,M., Wang,L.C., Kozekov,I.D., Rizzo,C.J., Gottesman,M.E. and Gautier,J. (2009) Checkpoint signaling from a single DNA interstrand crosslink. *Mol. Cell*, **35**, 704–715.
58. Sareen,A., Chaudhury,I., Adams,N. and Sobeck,A. (2012) Fanconi anemia proteins FANCD2 and FANCI exhibit different DNA damage responses during S-phase. *Nucleic Acids Res.*, **40**, 8425–8439.
59. Mordes,D.A. and Cortez,D. (2008) Activation of ATR and related PIKKs. *Cell Cycle*, **7**, 2809–2812.
60. Pace,P., Johnson,M., Tan,W.M., Mosedale,G., Sng,C., Hoatlin,M., de Winter,J., Joenje,H., Gergely,F. and Patel,K.J. (2002) FANCE: the link between Fanconi anaemia complex assembly and activity. *EMBO J.*, **21**, 3414–3423.
61. Cole,A.R., Lewis,L.P. and Walden,H. (2010) The structure of the catalytic subunit FANCL of the Fanconi anemia core complex. *Nat. Struct. Mol. Biol.*, **17**, 294–298.
62. Liu,S., Shiotani,B., Lahiri,M., Marechal,A., Tse,A., Leung,C.C., Glover,J.N., Yang,X.H. and Zou,L. (2011) ATR Autophosphorylation as a Molecular Switch for Checkpoint Activation. *Mol. Cell*, **43**, 192–202.
63. Pichierri,P., Franchitto,A. and Rosselli,F. (2004) BLM and the FANC proteins collaborate in a common pathway in response to stalled replication forks. *EMBO J.*, **23**, 3154–3163.

European Journal of Cancer (2013) 49, 3547–3558

Available at www.sciencedirect.com

SciVerse ScienceDirect

journal homepage: www.ejcancer.com

The HSP90 inhibitor 17-allylamino-17-demethoxygeldanamycin modulates radiosensitivity by downregulating serine/threonine kinase 38 via Sp1 inhibition

Atsushi Enomoto [a,*], Takemichi Fukasawa [a], Nobuhiko Takamatsu [b], Michihiko Ito [b], Akinori Morita [c], Yoshio Hosoi [c], Kiyoshi Miyagawa [a]

[a] *Laboratory of Molecular Radiology, Center for Disease Biology and Integrative Medicine, Graduate School of Medicine, The University of Tokyo, 7-3-1 Hongo, Bunkyo-ku, Tokyo 113-0033, Japan*

[b] *Department of Biosciences, School of Science, Kitasato University, 1-15-1 Kitasato, Sagamihara, Kanagawa 252-0373, Japan*

[c] *Department of Radiation Medicine, Research Center for Radiation Casualty Medicine, Research Institute for Radiation Biology and Medicine, Hiroshima University, 1-2-3 Kasumi, Minami-ku, Hiroshima 734-8553, Japan*

Available online 22 July 2013

KEYWORDS
17-AAG
STK38
Sp1
Radiosensitization

Abstract The ansamycin-based HSP90 inhibitor 17-AAG (17-allylamino-17-demethoxygeldanamycin) combats tumors and has been shown to modulate cellular sensitivity to radiation, prompting researchers to use 17-AAG as a radiosensitizer. 17-AAG causes the degradation of several oncogenic and signaling proteins. We previously demonstrated that oxidative stress activates serine/threonine kinase 38 (STK38), a member of the protein kinase A (PKA)/PKG/PKC-like family. In the present study, we investigated how 17-AAG affects STK38 expression, and evaluated STK38's role in the regulation of radiosensitivity. We found that 17-AAG depleted cellular STK38 and reduced STK38's kinase activity. Importantly, 17-AAG downregulated the *stk38* gene expression. Deletion analysis and site-directed mutagenesis experiments demonstrated that Sp1 was required for the *stk38* promoter activity. Treatment with 17-AAG inhibited Sp1's binding to the *stk38* promoter by decreasing the amount of Sp1 and knocking down Sp1 reduced STK38 expression. Moreover, 17-AAG treatment or STK38 knockdown enhanced the radiosensitivity of HeLa cells. Our data provide a novel mechanism, mediated by *stk38* downregulation, by which 17-AAG radiosensitizes cells.

* *Corresponding author:* Tel.: +81 (3) 5841 3505; fax: +81 (3) 5841 3013.
E-mail address: aenomoto-tky@umin.ac.jp (A. Enomoto).

0959-8049/$ - see front matter © 2013 Elsevier Ltd. All rights reserved.
http://dx.doi.org/10.1016/j.ejca.2013.06.034

1. Introduction

STK38 (serine/threonine kinase 38), also known as NDR1 (nuclear Dbf2-related 1; GenBank Accession No.: NP009202), is a serine/threonine protein kinase belonging to a subclass of the protein kinase A (PKA)/PKG/PKC-like (AGC) family,[1–3] which includes cAMP-dependent kinase, protein kinase B and protein kinase C. The STK38 family includes *Drosophila melanogaster* TRC, *Schizosaccharomyces pombe* Orb6, *Saccharomyces cerevisiae* Cbk1 and Dbf2 and mammalian STK38, STK38L/NDR2, LATS1 (large tumor suppressor 1), and LATS2.[1–3] Cbk1 and Orb6 regulate cell morphology.[4,5] Dbf2 is a cell cycle-regulated kinase required for the cycle to progress through anaphase.[6] STK38 and STK38L, which are broadly expressed in the mouse brain,[7] contribute to dendritic spine development and excitatory synaptic function.[8] STK38's activity is regulated by MST3 (mammalian sterile 20-like 3),[9] the cofactors MOB1 (Mps one binder 1) and MOB2,[10,11] or GSK-3 (glycogen synthase kinase-3).[12] We previously demonstrated that STK38 is involved in regulating MAPK (mitogen-activated protein kinase) signaling pathways and the oxidative stress response.[12,13]

Heat shock proteins (HSPs), a major class of molecular chaperones, play vital roles in cellular stress responses and cancer.[14] One particular chaperone, HSP90, dynamically promotes the conformational maturation of its client proteins and protects them from degradation by assembling client-HSP90 complexes using the chaperone machinery.[15,16] HSP90 is of considerable interest in the search for new therapeutic cancer targets, since most HSP90 client proteins are oncogenic proteins and protein kinases that regulate cell survival, proliferation, invasion, metastasis and angiogenesis.[14,17] The natural products radicicol and geldanamycin, along with their derivatives, combat tumors by inhibiting HSP90's intrinsic ATPase activity, causing HSP90's client proteins to be degraded via the ubiquitin–proteasome pathway.[18,19] The geldanamycin analogue 17-AAG (17-allylamino-17-demethoxygeldanamycin), a benzoquinone ansamycin, has similar anti-tumor properties and fewer associated side-effects.[20] In tumor cells, HSP90 is present in multi-chaperone complexes that have high ATPase activity and a strong binding affinity for 17-AAG. Since this is not the case in normal cells, 17-AAG is selective for tumors.[21] Studies have also shown that 17-AAG can radiosensitize tumor cells.[22,23]

Here we show that 17-AAG downregulates STK38 by inhibiting Sp1, and provide evidence that STK38 is a key factor in cellular sensitivity to ionizing radiation.

2. Materials and methods

2.1. Cell culture and stimulation

HeLa cells were purchased from the Japanese Collection of Research Bioresources Cell Bank (Ibaraki, Osaka). HCT116 cells were obtained from American Type Culture Collection (Manassas, VA). HEK293T and MCF-7 cells were gifts from Dr. Katsuji Yoshioka (Kanazawa University) and Dr. Kazuya Hirano (Tokyo University of Pharmacy and Life Sciences), respectively. HeLa, HEK293T, and MCF-7 cells were cultured in Dulbecco's modified Eagle's medium/F-12 (1:1) (Sigma, St. Louis, MO) supplemented with 10% fetal bovine serum (Hyclone, South Logan, UT) and 1% penicillin/streptomycin (Sigma). HCT116 cells were cultured in McCoy's 5A (Sigma) supplemented with 10% fetal bovine serum and 1% penicillin/streptomycin. Cells were treated with either dimethyl sulfoxide (DMSO) (Sigma) or 17-AAG (Sigma) for 2–16 h. For the combined treatment, HeLa cells were treated with either DMSO or 17-AAG for 12 h, X-ray-irradiated, incubated for an additional 2 h, harvested and assayed. MG132 (Sigma) and *clasto*-Lactacystin β-lactone (Calbiochem, Darmstadt, Germany) were stored as 10 mM stock solutions in DMSO and used at 10 μM. Cells were irradiated with an X-ray generator (Pantak HF 350, Shimadzu, Kyoto) operating at 200 kV–20 mA with a filter of 0.5 mm Cu and 1 mm Al at a dose rate of 1.46 Gy/min; 46 cm FSD.

2.2. Western blot analysis

Western blot analysis was performed as described previously.[13] Equivalent amounts of total cell lysates were separated by SDS–PAGE. Proteins separated in the gel were transblotted onto Immobilon PVDF membranes (Millipore, Bedford, MA). The membranes were blocked in Tris-buffered saline containing 0.05% Tween 20 (TBS-T) and 5% non-fat dry milk and incubated with anti-STK38,[13] anti-NDR1 (YJ-7, Santa Cruz Biotechnology, Santa Cruz, CA), anti-C/EBP beta (GeneTex, Irvine, CA) or anti β-Actin (Sigma) antibodies. The blots were triple-washed with TBS-T and incubated with secondary peroxidase-conjugated antibodies (Dako, Glostup, Denmark). Signals were detected on X-ray films (GE Healthcare, Buckinghamshire, UK) using an enhanced chemiluminescence detection system (GE Healthcare). STK38 was quantified using an LAS-1000 mini luminescent image analyzer (Fuji Film, Tokyo).

2.3. Immune-complex kinase assays

Cell lysates were prepared as described above, incubated with specific antibodies and mixed with protein A/G agarose. Immune-complex kinase assays were performed as described previously.[13]

2.4. Semi-quantitative RT-PCR analysis

Total RNA was isolated from cells treated with DMSO or 17-AAG using the Ultraspec RNA Isolation System (Biotecx Lab, Inc., Houston, TX). RNAs were

converted to cDNA using SuperScript III reverse transcriptase (Invitrogen Carlsbad, CA) and oligo(dT)$_{12-18}$ (GE Healthcare), and the cDNAs were amplified by polymerase chain reaction (PCR) using Pfx DNA polymerase (Invitrogen) and the following primer sequences:

stk38 (forward): ATGGCAATGACAGGCTCAAC ACCTTGCTC
stk38 (reverse): GCCTACTGTGGAGAAGGCTAG CTGACG.

Primers for β-actin were purchased from Stratagene (La Jolla, CA). PCR products were analyzed by electrophoresis on 2% agarose gels.

2.5. Plasmids

The *stk38* promoter (nt −877 to −11) was cloned by PCR using genomic DNA from HeLa cells as a template. Kpn I and Xho I sites were introduced into the forward and reverse primers, respectively, for cloning convenience. The PCR-amplified *stk38* fragment was digested with Kpn I and Xho I and ligated into the pGL3-Basic plasmid (Promega, Madison, WI). The 5′-region of the promoter was deleted by PCR. PCR fragments were subcloned into the pGL3-Basic plasmid as described above. Sp1-mutant constructs were generated using the GeneArt site-directed mutagenesis system (Invitrogen). The following mutated Sp1 oligonucleotide sequences were used:

Sp1 single-mutant forward: 5′-GGGGGTGAAGGGA GGGGCAGTTCGGGCCACGCAAGCGCAGT-3′
Sp1 single-mutant reverse: 5′-ACTGCGCTTGCGT GGCCCGAACTGCCCCTCCCTTCACCCCC-3′
Sp1 double-mutant forward: 5′-GCCCTAGGCA GGGGGTGAAGTTAGGGGCAG-3′
Sp1 double-mutant reverse: 5′-CCCGAACTGCCC CTAACTTCACCCCCTGCC-3′.

The mammalian STK38 short hairpin (sh) RNA expression vector was described previously.[13] All constructs were confirmed by sequencing.

2.6. Reporter assay

HeLa cells were plated onto 24-well plates at 1×10^4 cells/well, 1 day prior to transfection. The cells were transfected using FuGENE HD (Roche, Indianapolis, IN) with 50 ng pRL (*Renilla* luciferase)-SV40 and 1.0 μg pGL3 (*Firefly* luciferase) reporter plasmids containing the *stk38* promoter. Twenty-four hours after transfection, cell extracts were prepared and luciferase activity was measured, as described by the manufacturer of the reporter system (Promega). The luciferase activity was measured using a luminescencer (AB-2200; ATTO, Tokyo).

2.7. Cell-viability and colony-formation assays

To assay cell viability, HeLa cells were transiently transfected with either a non-targeting or an *stk38*-specific shRNA expression vector using FuGENE HD, double-washed 24 h later with Ca^{2+}/Mg^{2+}-free phosphate-buffered saline (PBS), and cultured for 48 h in medium containing 2 μg/ml puromycin (Invivogen, San Diego, CA). The cells were washed twice with PBS, left untreated or X-ray-irradiated at 3 Gy in the absence or presence of 17-AAG, and assayed for cell viability 48 h later by staining with Annexin V-FITC and propidium iodide (PI) using a MEBCYTO Apoptosis kit (MBL, Nagoya). Cell death was defined as the total percentage of cells positive for PI, Annexin V or both. All samples were counted, and more than 5000 cells were analyzed for each condition using a flow cytometer (EPICS XL System II, Beckman Coulter, Brea, CA).

Cell survival was measured by a colony-formation assay. HeLa cells were pretreated with 17-AAG or DMSO for 12 h, then X-ray-irradiated (0–5 Gy), trypsinized, diluted, counted and seeded into 60-mm dishes at various cell densities. After 7 days, the colonies were stained with crystal violet, and those containing more than 50 cells were counted. To determine the survival of STK38-knockdown cells, HeLa cells were transiently transfected with either a non-targeting or an *stk38*-specific shRNA expression vector, then selected with puromycin as described above, and assayed by colony formation. The X-ray dose-survival curves were fitted to a linear-quadratic (LQ) equation. The radiation enhancement ratio (RER) for 17-AAG or *stk38* knockdown was determined using the surviving fraction $SF_{0.5}$, determined from the clonogenic assay.

2.8. Preparation of nuclear extracts and gel-shift analysis

To prepare nuclear extracts, 1×10^7 HeLa cells were washed with PBS and suspended in 200 μl of hypotonic buffer A (10 mM Hepes–KOH, pH 7.9, 10 mM KCl, 0.2 mM EDTA, 0.4% NP-40, and 1 mM DTT) containing a protease inhibitor cocktail (Nacalai tesque). The suspension was incubated on ice for 10 min and then centrifuged at 1000*g* for 5 min to obtain nuclear pellets. The pellets were washed twice in ice-cold buffer A and resuspended in 100 μl of buffer B (20 mM Hepes–KOH, pH 7.9, 0.4 M NaCl, 2 mM EDTA, and 1 mM DTT) containing protease inhibitors. The suspension was incubated for 30 min on ice and then spun at 20,000*g* for 20 min. The supernatants were dialyzed against buffer C (20 mM Hepes–KOH pH 7.9, 50 mM KCl, and 1 mM DTT) containing protease inhibitors. Gel-shift assays were performed in a 10 μl final volume containing 4% glycerol, 1 mM $MgCl_2$, 0.5 mM DTT, 50 mM NaCl, 10 mM Tris–HCl, pH 7.5, and 0.25 μg of poly (dI–dC). Binding reactions were carried out

using 5.0 μg of nuclear extract and 1 μl of [^{32}P] dCTP-labeled probe at room temperature for 20 min. For competition assays, 10 μM unlabeled Sp1 consensus oligonucleotides (Promega) was added to the reaction mixture. For super-shift experiments, 1 μg of anti-Sp1 antibody (H-225, Santa Cruz Biotechnology) was added to the reaction mixture 10 min before adding the ^{32}P-labeled probe. The final reaction mixture was separated on a 5% non-denaturing polyacrylamide gel in 0.5× TBE at 350 V for 20 min. The following *stk38* promoter-specific oligonucleotides were used in the Sp1 gel-shift analysis:

*stk*38 wild-type: 5′-GGGGGTGAAGGGAGGGG-CAGGGCGGGGCCA-3′
*stk*38 single-mutant (sm): 5′- GGGGGTGAAGGG AGGGGCAGTTCGGGGCCA-3′
*stk*38 double-mutant (dm): 5′- GGGGGTGAAG TTAGGGGCAGTTCGGGGCCA-3′.

2.9. ChIP assay

For chromatin immunoprecipitation (ChIP) assays, 1×10^7 HeLa cells were treated with either DMSO or 17-AAG and fixed with 1.0% formaldehyde for 8 min at room temperature. The fixed cells were washed twice with ice-cold PBS and harvested with ice-cold PBS containing 1 mM PMSF. The cell pellets were resuspended in cell lysis buffer [50 mM Tris–HCl (pH 8.1), 1% SDS, 10 mM EDTA] containing protease inhibitor cocktail, and lysed on ice for 30 min. To shear chromatin DNA into 200–1000-bp lengths, the lysates were sonicated with five sets of 10-s pulses using a Branson Sonifier 150 W SLPe at 12% of maximum power. The sonicated lysates were then spun at 10,000*g* for 20 min. After measuring the DNA concentration of the sheared chromatin in the supernatants, the sheared chromatin was separated by electrophoresis, stained with ethidium bromide and visualized by UV emission. ChIP assays were performed using a ChIP assay kit (Upstate Biotechnology, Lake Placid, NY) according to the manufacturer's instructions, as follows: 2 μg of the sheared chromatin was immunoprecipitated with 1 μg of anti-Sp1 or anti-RNA polymerase II antibody (H-224, Santa Cruz Biotechnology) in ChIP dilution buffer (16.7 mM Tris–HCl, pH 8.1, 167 mM NaCl, 0.01% SDS, 1.1% Triton X-100, and 1.2 mM EDTA) containing a protease inhibitor cocktail. Sp1-associated or RNA polymerase II-associated DNA was amplified by PCR using the following promoter-specific primers:

stk38 (forward): 5′-ATGGTACCGAGGTAAGCT GGGTGGGTGATG-3′
stk38 (reverse): 5′-AAACTCGAGCGCGACTTCCC GGAGCGGCCG-3′
gapdh (forward): 5′-TACTAGCGGTTTTACGG GCG-3′
gapdh (reverse): 5′-TCGAACAGGAGGAGCAGA-GAGCGA-3′.

PCR products were separated by electrophoresis through a 2% agarose gel, stained with ethidium bromide and visualized by UV emission.

3. Results

3.1. 17-AAG treatment reduces STK38 protein levels

We previously demonstrated that oxidative stress stimulates STK38, and that STK38 activation is required to protect cells from oxidative stress.[12] Those findings, along with reports that inhibiting HSP90 enhances the cellular sensitivity to oxidative stresses by degrading or downregulating signaling proteins,[14,22,23] led us to investigate whether inhibiting HSP90 affects STK38 expression. Treating cells with an HSP90 inhibitor provides a simple assay of whether a given protein depends on HSP90 activity, either directly or indirectly. Thus, we examined if the HSP90 inhibitor 17-AAG affected STK38 in HeLa cells, and found that the endogenous STK38 protein decreased according to 17-AAG dosage (Fig. 1A). A concentration of 1 μM 17-AAG, at which HSP90 is fully inhibited in various cell lines,[24] was maximally effective for depleting STK38. We next treated cells with 0.5 μM 17-AAG for various times, and found a time-dependent decrease in the STK38 level (Fig. 1B). The effect of 17-AAG on STK38 was similar in HEK293T, HCT116 and MCF7 cells (Fig. 1C). We also found that the kinase activity of immunoprecipitated endogenous STK38 was decreased by 17-AAG in a dose-dependent manner (Fig. 1D), probably because the expression level of STK38 was reduced.

3.2. Expression of the stk38 gene is downregulated by 17-AAG

The inhibition of HSP90 disturbs its client proteins by disrupting their chaperoning and targeting them for proteasomal degradation. We next investigated whether the ubiquitin–proteasome system is responsible for depleting STK38 when HSP90's activity is inhibited. Surprisingly, treating HeLa cells with proteasome inhibitors, 10 μM MG132 or 10 μM lactacystin, did not antagonize the 17-AAG-induced STK38 depletion (Fig. 2A). Since these findings suggested that STK38 is not degraded by the ubiquitin–proteasome pathway, we assessed the effect of 17-AAG on *stk38* gene expression using semi-quantitative RT-PCR. As shown in Fig. 2B and C, 17-AAG downregulated the *stk38* mRNA in a dose- and time-dependent manner.

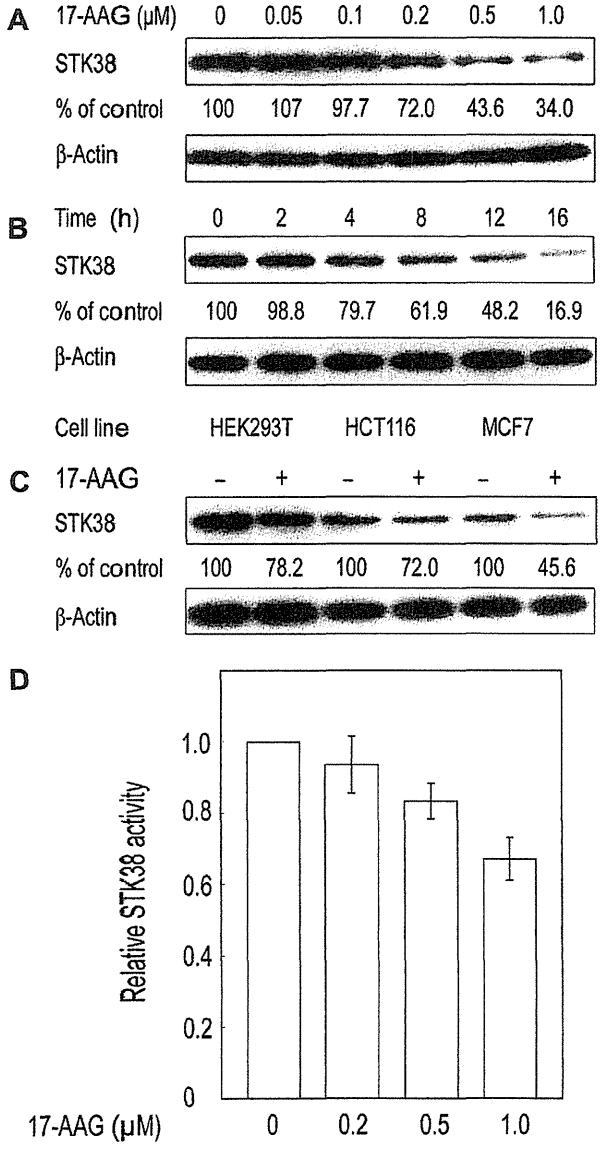

Fig. 1. Treatment with 17-allylamino-17-demethoxygeldanamycin (17-AAG) decreased serine/threonine kinase 38 (STK38) expression. (A) HeLa cells were treated with dimethyl sulfoxide (DMSO) (vehicle) or various concentrations of 17-AAG for 12 h. (B) HeLa cells were treated with 0.5 μM 17-AAG for the times indicated. (C) Various cell lines were treated with 0.5 μM 17-AAG for 12 h, then cell lysates were analyzed by Western blot with the indicated antibodies. STK38 signals were quantified and normalised against β-actin signals. (D) HeLa cells were treated with DMSO or various concentrations of 17-AAG for 12 h. STK38 kinase activity was measured in cell lysates by immune-complex kinase assay with an anti-STK38 antibody, using a synthetic peptide as the substrate. Data represent the average and standard deviations of three independent experiments, expressed as STK38 activity relative to that of DMSO-treated cells.

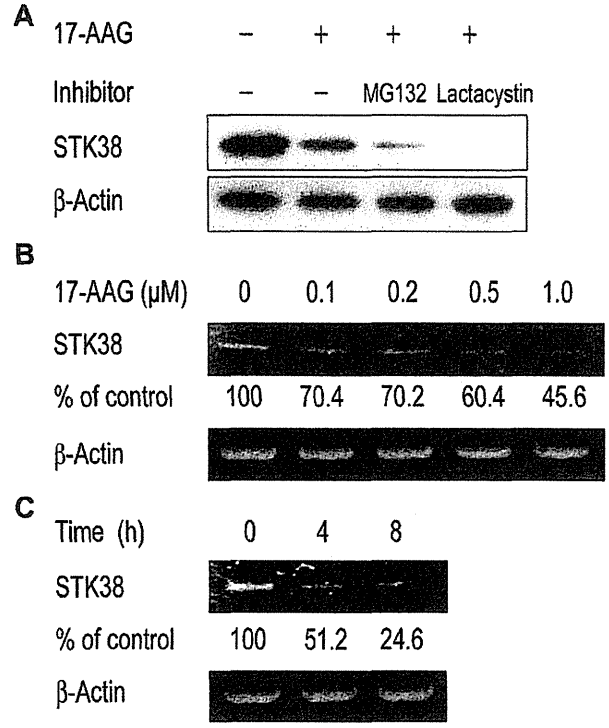

Fig. 2. Treatment with 17-allylamino-17-demethoxygeldanamycin (17-AAG) downregulated the *stk38* expression. (A) Proteasome inhibitors did not block 17-AAG-mediated serine/threonine kinase 38 (STK38) depletion. HeLa cells were treated for 12 h with 0.5 μM 17-AAG, either alone or with 10 μM MG132 or lactacystin, then cell lysates were analyzed by Western blot with the indicated antibodies. (B) HeLa cells were treated with DMSO or various concentrations of 17-AAG for 12 h. (C) HeLa cells were treated with 0.5 μM 17-AAG for the indicated times. Total RNA was prepared from treated and untreated cells, and *stk38* mRNA levels were estimated by semi-quantitative RT-PCR. STK38 signals were quantified and normalised against β-actin signals.

3.3. Sp1-dependent regulation of the stk38 promoter

To investigate how the human *stk38* gene is regulated, we constructed a luciferase reporter plasmid containing the 5′-flanking region (nt −877 to −11) of the human *stk38* gene, containing its promoter. Since computational predictive analysis of the region revealed putative consensus sequences for NF-κB, CREB, C/EBP, Sp1 and Ap1 (Fig. 3A), we applied stimuli to activate these transcriptional factors and measured their subsequent luciferase activity. However, treatment with TNF-α or Forskolin, which respectively stimulate NF-κB and CREB activity, did not significantly alter the luciferase activity driven by the *stk38* promoter (see Supplemental Fig. 1). We next constructed reporter plasmids containing 5′-serial deletions of the *stk38* promoter and measured their activity. The promoter's basal activity did not vary with deletions in the region between −877 and −280 (Fig. 3B). Deleting the region between −280 and −277 reduced the luciferase activity to 57% of that of the *stk38* promoter containing the 5′-flanking region between −877 and −11, suggesting the involvement of a transcriptional factor in the −280/−277 region. Computational analysis of this region predicted the existence of an Ap1-binding site. However, PMA, an Ap1 activator, did not stimulate the *stk38* promoter activity (Supplemental Fig. 1).